T668-phosphorylated APP cytoplasmic domain accumulates in the tau Tg mice

The immunohistochemical examination of AD and non-AD control brains shows that neuronal cells affected by tau accumulation exhibit co-accumulation of pT668-ACD, while normal neuronal cells unaffected by tau accumulation lack accumulation of pT668-ACD. Thus, it appears that there is an association between neuronal accumulations of tau and pT668-ACD. To study the relationship between these abnormal accumulates, we examined the brains of the old tau Tg mice in which overexpressed transgenic tau accumulates in a certain population of neuronal cells [14]. The brain sections immunostained by PHF1 displayed affected neuronal cells and neuropil threads that induce tau accumulation (Fig. 5a, c). In the adjacent sections immunostained by anti-pT668, a significant proportion of the neuronal cells with tau aggregates contained accumulated pT668-ACD, and a less density of the neuropil threads appeared to contain accumulated pT668-ACD (Fig. 5b, d). Thus, the neuronal cells affected by tau accumulation induce co-accumulation of pT668-ACD. By analogy, it is also likely that in AD brain degenerating neuronal cells with tau accumulation may induce co-accumulation of pT668-ACD.

Discussion

The present study has revealed the potential role of APP cytoplasmic domain with phosphorylated T668 (pT668-ACD) as a molecular factor that associates with and links Aβ and tau accumulating as SPs and NFTs, respectively, the main pathological features of AD. We demonstrate that pT668-ACD accumulates in the dystrophic neurites of mature SPs and in the neuronal cells affected by the formation of NFTs, in accordance with the previous study [19]. In these pathological entities, accumulation of pT668-ACD occurs in association, but without colocalization with Aβ, while it occurs in colocalization with tau. Aβ is the proteolytic product of membrane-associated APP and is secreted into the extracellular space, while APP cytoplasmic domain is confined to the cytosol, where microtubule-associated protein tau exists. Thus, under pathological conditions of AD, intracellular accumulation of pT668-ACD occurs and is reasonably colocalized with intracellular tau, but not with extracellular Aβ.

Phosphorylation at T668 of APP regulates APP processing in such a way as to increase Aβ production [1, 3, 19], indicating that Aβ production and T668 phosphorylation of APP are linked. However, T668A mutant of APP still yields Aβ, albeit less efficiently, indicating that APP unphosphorylated at T668 is also available for Aβ production. Thus, there might be two alternative pathways whereby APP produces Aβ, T668 phosphorylation-dependent and -independent Aβ productions. It is likely that these two different pathways underlie separately the formation of the mature plaques with surrounding dystrophic neurites and the diffuse plaques without dystrophic neurites: the T668 phosphorylation-dependent Aβ production is associated with the formation of the mature plaques, where Aβ and pT668-ACD co-accumulate; while T668 phosphorylation-independent Aβ production is associated with the formation of the diffuse plaques, where Aβ, but not pT668-ACD, accumulates. In the APP-SL and Tg2576 mice, Aβ

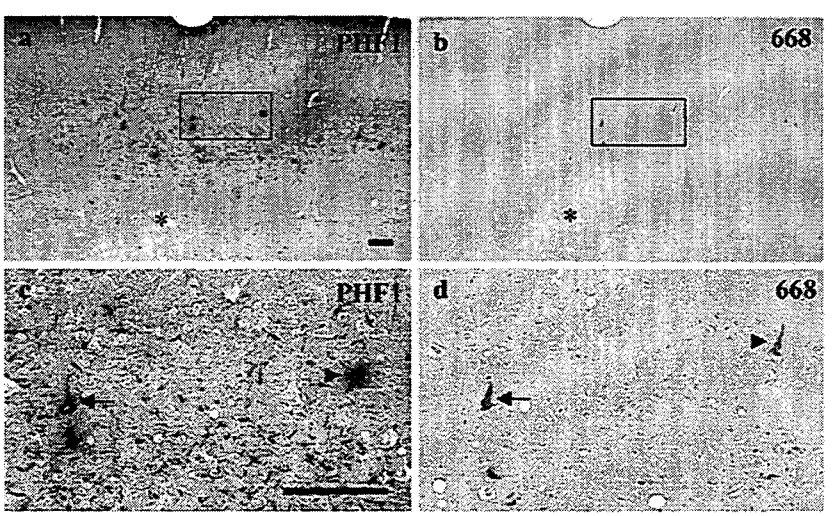

Fig. 5 Co-accumulation of pT668-ACD with tau in affected neuronal cells of the brain from a 32-month-old tau transgenic mouse. Immunohistochemistry of the serial brain sections using PHF1 (**a**) and anti-pT668 (668) (**b**). **c**, **d** higher magnification pictures of areas outlined by *squares* in **a** and **b**, respectively. *Arrow* and *arrowhead* denote neuronal cells affected by co-accumulation of tau and pT668-ACD. *Asterisk* (*) denotes a landmark vessel to indicate the serial sections. **a**, **b** and **c**, **d** are at the same magnifications, respectively. *Scale bars* 100 μM (**a**, **c**)

plaques formed in the cortex and cerebellum show co-accumulation of pT668-ACD, and therefore the T668 phosphorylation-dependent pathway might be primarily responsible for the production of Aβ in these mutant APP Tg mice.

Among the phosphorylated sites described on the cytoplasmic domain of APP, T668 is of considerable interest. This phosphorylation site was suggested to be the target of protein kinases in common with those involved in the phosphorylation of tau, the major constituent of the NFTs and SP dystrophic neurites in AD, i.e., CDK5, GSK3β and SPK/JNK [4, 8, 12, 13, 32]. In these pathological entities, tau and pT668-ACD co-accumulate and colocalize with each other, suggesting mechanistic and functional link between them. Use of the transgenic models for SPs and those for NFTs helped to give insight into the relationships between accumulations of tau and pT668-ACD. In the APP-SL and Tg2576 mice, deposition of Aβ is accompanied by co-accumulation of pT668-ACD prior to that of tau. In the tau Tg mice, neuronal cells affected by tau accumulation show co-accumulation of pT668-ACD. By analogy of these phenomena seen in the AD models, it is likely that in AD, the extracellular deposition of Aβ causes surrounding neurites dystrophic, wherein pT668-ACD accumulation occurs and is followed by tau accumulation forming the mature SPs, while neuronal cells with tau aggregates induce co-accumulation of pT668-ACD, forming the NFTs. Thus, there might be reciprocal relationships between pathological accumulations of pT668-ACD and tau.

Intraneuronal accumulation of ubiquitinated protein aggregates is a common feature of the major human neurodegenerative disorders, including AD and Parkison's disease. The target substrates are the disease-characteristic proteins that constitute the hallmark lesions, such as phosphorylated tau [21, 22] and phosphorylated α-synuclein of Lewy bodies characteristic to Parkinson's disease [15]. Herein, we provided evidence for a possibility that T668-phosphorylated APP cytoplasmic domain co-accumulating with tau is also ubiquitinated. Indeed the cytoplasmic domain of APP has several lysine sites potential for ubiquitination, and we observed that β-cleaved C-terminal APP including the cytoplasmic domain is polyubiquitinated (unpublished data). As accumulations of ubiquitinated protein aggregates reflect failed attempts by the ubiquitin-proteasome system to remove pathological proteins [7], the roles of ubiquitinated pT668-ACD as well as ubiquitinated tau and α-synuclein in the disease process remain to be determined.

Acknowledgments We thank Dr. J. Q. Trojanowski and V.M.-Y. Lee for providing the brain samples of the tau transgenic mice, Drs. P. Davies and S. Greenberg for providing PHF1, Dr. T. Suzuki for UT-18, and Dr. H. Sato for BE11. We also thank Ms. H. Kudo, Ms. K. Abe and Ms. A. Yamazaki for technical assistance. This study was supported by a grant from the Ministry of Health, Labor, and Welfare, Japan; and grants-in-aid for scientific research from the Ministry of Education, Culture, Sports, Science, and Technology, Japan.

References

1. Akiyama H, Shin R-W, Uchida C, Kitamoto T, Uchida T (2005) Pin1 promotes production of Alzheimer's amyloid beta from beta-cleaved amyloid precursor protein. Biochem Biophys Res Commun 336:521–529
2. Alvarez A, Toro R, Caceres A, Maccioni RB (1999) Inhibition of tau phosphorylating protein kinase cdk5 prevents beta-amyloid-induced neuronal death. FEBS Lett 459:421–426
3. Ando K, Iijima KI, Elliott JI, Kirino Y, Suzuki T (2001) Phosphorylation-dependent regulation of the interaction of amyloid precursor protein with Fe65 affects the production of beta-amyloid. J Biol Chem 276:40353–4036
4. Aplin AE, Gibb GM, Jacobsen JS, Gallo J-M, Anderton BH (1996) In vitro phosphorylation of the cytoplasmic domain of the amyloid precursor protein by glycogen synthase kinase-3β. J Neurochem 67:699–707
5. Arai H, Lee VM, Otvos L Jr, Greenberg BD, Lowery DE, Sharma SK, Schmidt ML, Trojanowski JQ (1990) Defined neurofilament, tau, and beta-amyloid precursor protein epitopes distinguish Alzheimer from non-Alzheimer senile plaques Proc Natl Acad Sci USA 87:2249–2253
6. Busciglio J, Lorenzo A, Yeh J, Yankner BA (1995) beta-amyloid fibrils induce tau phosphorylation and loss of microtubule binding. Neuron 14:879–888
7. Ciechanover A, Brundin P (2003) The ubiquitin proteasome system in neurodegenerative diseases: sometimes the chicken, sometimes the egg. Neuron 40:427–446
8. Goedert M, Hasegawa M, Jakes R, Lawler S, Cuenda A, Cohen P (1997) Phosphorylation of microtubule-associated protein tau by stress-activated protein kinases. FEBS Lett 409:57–62
9. Gotz J, Chen F, van Dorpe J, Nitsch RM (2001) Formation of neurofibrillary tangles in P3011 tau transgenic mice induced by Aβ 42 fibrils. Science 293:1491–1495
10. Greenberg SG, Davies P, Schein JD, Binder LI (1992) Hydrofluoric acid-treated tau PHF proteins display the same biochemical properties as normal tau. J Biol Chem 267:564–569
11. Hsiao K, Chapman P, Nilsen S, Eckman C, Harigaya Y, Younkin S, Yang F, Cole G (1996) Correlative memory deficits, Aβ elevation, and amyloid plaques in transgenic mice. Science 274:99–102
12. Iijima K, Ando K, Takeda S, Satoh Y, Seki T, Itohara S, Greengard P, Kirino Y, Nairn AC, Suzuki T (2000) Neuron-specific phosphorylation of Alzheimer's beta-amyloid precursor protein by cyclin-dependent kinase 5. J Neurochem 75:1085–1091
13. Imahori K, Uchida T (1997) Physiology and pathology of tau protein kinases in relation to Alzheimer's disease. J Biochem (Tokyo) 121:179–188
14. Ishihara T, Zhang B, Higuchi M, Yoshiyama Y, Trojanowski JQ, Lee VM (2001) Age-dependent induction of congophilic neurofibrillary tau inclusions in tau transgenic mice. Am J Pathol 158:555–562
15. Iwatsubo T, Yamaguchi H, Fujimuro M, Yokosawa H, Ihara Y, Trojanowski JQ, Lee VM (1996) Purification and characterization of Lewy bodies from the brains of patients with diffuse Lewy body disease. Am J Pathol 148:1517–1529
16. Kitamoto T, Ogomori K, Tateishi J, Prusiner SB (1987) Formic acid pretreatment enhances immunostaining of cerebral and systemic amyloids. Lab Invest 57:230–236
17. Kitamoto T, Mohri S, Ironside JW, Miyoshi I, Tanaka T, Kitamoto N, Itohara S, Kasai N, Katsuki M, Higuchi J, Muramoto T, Shin R-W

(2002) Follicular dendritic cell of the knock-in mouse provides a new bioassay for human prions. Biochem Biophys Res Commun 294:280–286
18. Lang E, Szendrei GI, Lee VM-Y, Otvos L Jr (1992) Immunological and conformation characterization of a phosphorylated immunodominant epitope on the paired helical filaments found in Alzheimer's disease. Biochem Biophys Res Commun 187:783–790
19. Lee MS, Kao SC, Lemere CA, Xia W, Tseng HC, Zhou Y, Neve R, Ahlijanian MK, Tsai LH (2003) APP processing is regulated by cytoplasmic phosphorylation. J Cell Biol 163:83–95
20. Lewis J, Dickson DW, Lin WL, Chisholm L, Corral A, Jones G, Yen SH, Sahara N, Skipper L, Yager D, Eckman C, Hardy J, Hutton M, McGowan E (2001) Enhanced neurofibrillary degeneration in transgenic mice expressing mutant tau and APP. Science 293:1487–1491
21. Mori H, Kondo J, Ihara Y (1987) Ubiquitin is a component of paired helical filaments in Alzheimer's disease. Science 235:1641–1644
22. Morishima-Kawashima M, Hasegawa M, Takio K, Suzuki M, Titani K, Ihara Y (1993) Ubiquitin is conjugated with amino-terminally processed tau in paired helical filaments. Neuron 10:1151–1160
23. Murayama H, Shin R-W, Higuchi J, Shibuya S, Muramoto T, Kitamoto T (1999) Interaction of aluminum with PHFtau in Alzheimer's disease neurofibrillary degeneration evidenced by desferrioxamine-assisted chelating autoclave method. Am J Pathol 155:877–885
24. Oishi M, Nairn AC, Czernik AJ, Lim GS, Isohara T, Gandy SE, Greengard P, Suzuki T (1997) The cytoplasmic domain of Alzheimer's amyloid precursor protein is phosphorylated at Thr654, Ser655, and Thr668 in adult rat brain and cultured cells. Mol Med 3:111–123
25. Sato H, Hirata J, Furukawa M, Kuroda N, Shiraki H, Maeda Y, Okochi K (1991) Identification of the region including the epitope for a monoclonal antibody which can neutralize human parvovirus B19. J Virol 65:1667–1672
26. Selkoe DJ (2001) Alzheimer's disease: genes, proteins, and therapy. Physiol Rev 81:741–766
27. Shin R-W, Ogomori K, Kitamoto T, Tateishi J (1989) Increased tau accumulation in senile plaques as a hallmark in Alzheimer's disease. Am J Pathol 134:1365–1371
28. Shin R-W, Iwaki T, Kitamoto T, Tateishi J (1991) Hydrated autoclave pretreatment enhances tau immunoreactivity in formalin-fixed normal and Alzheimer's disease brain tissues. Lab Invest 64:693–702
29. Shin R-W, Iwaki T, Kitamoto T, Sato Y, Tateishi J (1992) Massive accumulation of modified tau and severe depletion of normal tau characterize the cerebral cortex and white matter of Alzheimer's disease. Demonstration using the hydrated autoclaving method. Am J Pathol 140:937–945
30. Shin R-W, Bramblett GT, Lee VM-Y, Trojanowski JQ (1993) Alzheimer disease A68 proteins injected into rat brain induce co-deposits of β-amyloid, ubiquitin, and α1-antichymotrypsin. Proc Natl Acad Sci USA 90:6825–6828
31. Shin R-W, Saido TC, Maeda M, Kitamoto T (2005) Novel α-secretase cleavage of Alzheimer's amyloid beta precursor protein in the endoplasmic reticulum of COS7 cells. Neurosci Lett 376:14–19
32. Standen CL, Brownlees J, Grierson AJ, Kesavapany S, Lau K-F, McLoughlin DM, Miller CCJ (2001) Phosphorylation of thr (668) in the cytoplasmic domain of the Alzheimer's disease amyloid precursor protein by stress-activated protein kinase 1b (Jun N-terminal kinase-3). J Neurochem 76:316–320
33. Takashima A, Honda T, Yasutake K, Michel G, Murayama O, Murayama M, KIshiguro K, Yamaguchi H (1998) Activation of tau protein kinase I/glycogen synthase kinase-3β by amyloid β peptide (25–35) enhances phosphorylation of tau in hippocampal neurons. Neurosci Res 31:317–323
34. Tomita S, Ozaki T, Taru H, Oguchi S, Takeda S, Yagi Y, Sakiyama S, Kirino Y, Suzuki T (1999) Interaction of a neuron-specific protein containing PDZ domains with Alzheimer's amyloid precursor protein. J Biol Chem 274:2243–2254
35. Weidemann A, Konig G, Bunke D, Fischer P, J. Salbaum M, C.L. Masters CL, Beyreuther K (1989) Identification, biogenesis, and localization of precursor of Alzheimer's disease A4 amyloid protein. Cell 57:115–126

Ophthalmic Surgery in Prion Diseases

Tsuyoshi Hamaguchi,[*1] Moeko Noguchi-Shinohara,[*] Yosikazu Nakamura,[†2] Takeshi Sato,[‡2] Tetsuyuki Kitamoto,[§2] Hidehiro Mizusawa,[¶2] and Masahito Yamada[*2]

Eleven (1.8%) of 597 patients underwent ophthalmic surgery within 1 month before the onset of prion disease or after the onset. All ophthalmologists reused surgical instruments that had been incompletely sterilized to eliminate infectious prion protein. Ophthalmologists should be aware of prion diseases as a possible cause of visual symptoms and use disposable instruments whenever possible.

Visual impairment occurs in 10% to 20% of patients with sporadic Creutzfeldt-Jakob disease (sCJD) during an early stage of the disease (Heidenhain variant) (*1,2*). Some patients with prion diseases may visit ophthalmologists with visual impairment due to prion diseases or with coexisting age-related eye diseases (*3,4*).

Infectious prion protein (PrP^{Sc}) was identified in the retina and optic nerve in patients with variant CJD (vCJD) and sCJD (*5,6*), and CJD has been transmitted by corneal transplantation (*7,8*). In the World Health Organization (WHO) guidelines, eyes were classified as highly infectious tissues (*9*).

Secondary transmission of PrP^{Sc} through ophthalmic surgery could possibly be prevented around the onset of prion diseases, although surgery that is performed long before the onset of prion diseases would not have that potential. It is important to understand the current status of ophthalmic surgery for patients with prion diseases and to clarify the clinical features of the patients with prion diseases who undergo ophthalmic surgery. Here, we describe the relevant data from CJD surveillance in Japan.

The Study

We analyzed the patients with prion diseases who had been registered by the CJD Surveillance Committee in Japan from April 1999 through March 2005. We prospectively investigated each patient with a surveillance protocol that assembled information about life history, previous medical history, clinical history, laboratory data, and results of molecular genetic and pathologic analyses. Written consent, approved by the Institutional Ethics Committee, was obtained from all the patients' families; members of the Surveillance Committee examined the patients and collected the data.

We classified the patients into 4 categories: sCJD, infectious prion diseases, inherited prion diseases, and unclassified prion diseases. sCJD was diagnosed according to the classical criteria established by Masters et al. (*10*). Infectious prion diseases included CJD associated with cadaveric dura mater graft (dCJD) or other iatrogenic opportunities for prion infection, in which the criteria for sCJD were applied for the diagnosis, and vCJD, in which the diagnosis was based on WHO criteria (2001) (*11*). Regarding the accuracy of the diagnosis of inherited prion diseases, cases verified by pathology report were defined as definite, and cases with mutations in the prion protein gene and neuropsychiatric manifestations compatible with prion diseases were defined as probable.

Among patients with a history of ophthalmic surgery, we directed special attention to the patients who had a history of eye surgery within 1 month before the obvious onset of prion disease or after the onset. Because the onset of prion diseases often overlaps with various kinds of prodromal symptoms, determining the precise time point of onset is difficult; therefore, we included the period of 1 month before the obvious onset. To gather information about the ophthalmic surgery, we mailed questionnaires to the ophthalmologists who operated on these patients, requesting the following information: diagnosis of ophthalmologic diseases, surgical procedures performed, changes in the symptoms after the surgery, whether the instruments were reused, and methods of cleaning reused instruments.

To ascertain the clinical features of prion diseases, we analyzed the patient's age at onset and duration of disease course, which was calculated as the interval between the onset and the appearance of the akinetic mutism state or death in the patients who died without akinetic mutism. Among early clinical manifestations of prion diseases, dementia and visual disturbance are major determinants that would influence the indication for ophthalmic surgery, so we grouped the patients according to whether they had dementia or visual impairment within 2 months after onset of symptoms.

The sex distribution of the patients who had ophthalmic surgery around the time of onset of clinical symp-

*Kanazawa University Graduate School of Medical Science, Kanazawa, Japan; †Jichi Medical University, Shimotsuke, Japan ‡National Center for Neurology and Psychiatry, Ichikawa, Japan; §Tohoku University Graduate School of Medicine, Sendai, Japan; and ¶Tokyo Medical and Dental University, Tokyo, Japan

[1]Current affiliation: Ishikawa Prefecture Central Hospital, Kanazawa, Japan

[2]Member, Creutzfeldt-Jakob Disease Surveillance Committee, Japan

toms and those who did not was compared by Fisher exact tests, and differences in age at onset and disease duration were compared by Mann-Whitney U tests. We used χ^2 tests to compare the distribution of the patients with or without dementia or visual impairment within 2 months of onset. Statistical significance was defined as $p<0.05$.

We found 597 patients with definite or probable diagnosis of prion diseases: 468 (78.4%) with sCJD; 78 (13.1%) with inherited prion diseases; 48 (8.0%) with infectious prion diseases, including 47 cases of dCJD; and 1 patient with vCJD and 3 patients with unclassified CJD.

Thirty-seven patients (6.2%) had a history of ophthalmic surgery at some time in their lives. Among them, 11 patients (1.8%) underwent ophthalmic surgery within 1 month before the obvious onset of prion disease or after the onset. Except for 1 patient with Gerstmann-Sträussler-Scheinker disease, all of these patients had sCJD. There have been no reports of the development of prion diseases in patients who underwent ophthalmic surgery after the ophthalmic surgery of patients with prion diseases.

Ten patients with sCJD underwent ophthalmic surgery within 14 months of symptom onset, and 8 of them had ophthalmic surgery within 4 months of symptom onset (Table 1). At clinical onset, 4 patients exhibited visual symptoms, 5 had dementia, and 1 patient had a gait disturbance. All patients underwent surgery for cataracts, except for 1 patient who underwent surgery for a detached retina. According to the reports on the surgical outcome by the ophthalmologists of 7 patients, visual disturbance was unchanged in 2 patients, deteriorated in 1, and improved to some extent in 4 after surgery. All ophthalmologists reused some surgical instruments and cleaned instruments by either autoclaving or the ethylene oxide gas method, which have been reported to incompletely sterilize PrP^{Sc} (*9*,*12*).

Clinical features were compared between sCJD patients who did and did not have ophthalmic surgery (Table 2). The patients who had ophthalmic surgery had a significantly longer disease duration than those without ($p=0.0004$). Regarding early clinical symptoms within 2 months after onset, the subgroup with visual symptoms without dementia was significantly overrepresented among the patients who had ophthalmic surgery compared with those who did not have surgery ($p= 0.0004$).

Conclusions

Our study showed that, in 1.8% of the patients with prion diseases, eye tissues were operated on within 1 month before the obvious onset of prion disease or after the onset. In addition, the sCJD patients who underwent surgery had a significantly longer duration of the disease course as well as significant overrepresentation of visual symptoms without dementia in the early phase, compared with patients who did not have ophthalmic surgery.

The prevalence of ophthalmic surgery around the time of clinical onset of prion diseases in our study is similar to that (2.0%) in a report from the United Kingdom (*13*). In the UK study (*13*), patients with Heidenhain variant cases constituted 40% of sCJD patients who had ophthalmic surgery. Early visual impairment (due to prion diseases) would prompt ophthalmologists to perform surgery.

Currently, cataract surgery is recommended to improve physical or cognitive function in elderly patients (*14*,*15*). It should be noted that, after performing eye surgery on patients with prion disease, all ophthalmologists reused surgical instruments that were sterilized with procedures that are incomplete for the sterilization of PrP^{Sc}, although the WHO infection control guidelines for prion diseases (*9*) strongly recommend single-use surgical

Table 1. Characteristics of sCJD patients and ophthalmic surgery*

Patient no.	Sex/age, y†	Disease duration, mo‡	Symptom at sCJD onset	Ophthalmic disease	Interval, mo§	Visual symptoms after surgery	Reused instruments	Cleaning method
1	M/81	8	Visual	Cataract	4	NA	NA	NA
2	M/61	15	Dementia	Cataract	0	Improved	Yes	Autoclave (135°C for 9 min)
3	F/64	20	Visual	Cataract	14	Not changed	Yes	EOG
4	F/59	3	Dementia	Detached retina	−1	Improved	Yes	EOG
5	F/57	10	Dementia	Cataract	10	NA	NA	NA
6	F/79	5	Dementia	Cataract	−1	Improved	Yes	EOG
7	M/74	16	Visual	Cataract	3	Improved	Yes	Autoclave (132°C for 10 min), EOG
8	F/63	5	Visual	Cataract	1	Deteriorated	Yes	Autoclave (132°C for 10 min)
9	M/79	6	Gait disturbance	Cataract	2	Not changed	Yes	Autoclave (121°C for 60 min)
10	F/66	3	Dementia	Cataract	1	NA	NA	NA

*sCJD, sporadic Creutzfeldt-Jakob disease; visual, visual impairment; NA, not available; EOG, ethylene oxide gas.
†At sCJD onset.
‡Disease duration, the duration from onset to akinetic mutism state or death if the patients never displayed akinetic mutism.
§Between surgery and sCJD symptoms.

Table 2. Clinical symptoms of sCJD within 2 mo after disease onset*

Characteristic	Ophthalmic surgery		Total	p value
	No, n = 458	Yes, n = 10		
Female/male	263/195	6/4	269/199	0.57
Age at onset, y; mean ± SD	66.8 ± 9.9	68.3 ± 9.1	66.8 ± 9.9	0.74
Disease duration,† mean ± SD	4.2 ± 4.8	9.1 ± 6.0	4.3 ± 4.9	0.0004
Clinical symptoms (%)				
Dementia (+)/visual impairment (+)	153 (34.2)	4 (40.0)	157 (34.3)	
Dementia (+)/visual impairment (–)	239 (53.3)	3 (30.0)	242 (52.8)	0.0004
Dementia (–)/visual impairment (+)	16 (3.6)	3 (30.0)	19 (4.1)	
Dementia (–)/visual impairment (–)	40 (8.9)	0	40 (8.7)	

*sCJD, sporadic Creutzfeldt-Jakob disease; SD, standard deviation; +, with; –, without.
†Disease duration, the duration from onset to akinetic mutism or death if patients never displayed akinetic mutism.

instruments for procedures involving highly infective tissues. The fact that no secondary iatrogenic cases that could be attributed to surgical procedures were found during our investigation does not diminish the need for ophthalmologists to be aware of CJD as a cause of visual symptoms (including symptoms mimicking those of cataracts) and highlight the importance of using disposable instruments whenever possible to avoid cross-contamination.

Acknowledgments

We thank Fumio Moriwaka, Yoshiyuki Kuroiwa, Masatoyo Nishizawa, Nobuyuki Sodeyama, Masatoshi Takeda, Yusei Shiga, Shigetoshi Kuroda, Shigeki Kuzuhara, Jun Tateishi, Hiroyuki Murai, and Shigeo Murayama for the CJD surveillance.

The CJD Surveillance Committee belongs to the Research Group on Prion Disease and Slow Virus Infection, funded by the Ministry of Health, Labour and Welfare, Japan; the funding source had no involvement in the publication of this article.

Dr Hamaguchi is a clinical research fellow in the Department of Neurology and Neurobiology of Aging, Kanazawa University Graduate School of Medical Science, Kanazawa, Japan. His primary research interest is prion diseases.

References

1. Kropp S, Schulz-Schaeffer WJ, Finkenstaedt M, Riedemann C, Windl O, Steinhoff BJ, et al. The Heidenhain variant of Creutzfeldt-Jakob disease. Arch Neurol. 1999;56:55–61.
2. Lueck CJ, McIlwain GG, Zeidler M. Creutzfeldt-Jakob disease and the eye. II. Ophthalmic and neuro-ophthalmic features. Eye. 2000;14:291–300.
3. Cooper SA, Murray KL, Heath CA, Will RG, Knight RSG. Isolated visual symptoms at onset in sporadic Creutzfeldt-Jakob disease: the clinical phenotype of the "Heidenhain variant." Br J Ophthalmol. 2005;89:1341–2.
4. Tullo A. Creutzfeldt-Jakob disease and eye surgery—new disease, old disease. J Cataract Refract Surg. 2003;29:629–31.
5. Head MW, Northcott V, Rennison K, Ritchie D, McCardle L, Bunn TJ, et al. Prion protein accumulation in eyes of patients with sporadic and variant Creutzfeldt-Jakob disease. Invest Ophthalmol Vis Sci. 2003;44:342–6.
6. Head MW, Peden AH, Yull HM, Ritchie DL, Bonshek RE, Tullo AB, et al. Abnormal prion protein in the retina of the most commonly occurring subtype of sporadic Creutzfeldt-Jakob disease. Br J Ophthalmol. 2005;89:1131–3.
7. Duffy P, Wolf J, Collins G, DeVoe AG, Sreeten B, Cowen D. Possible person-to-person transmission of Creutzfeldt-Jakob disease. N Engl J Med. 1974;290:692–3.
8. Heckmann JG, Lang CJG, Petruch F, Druschky A, Erb C, Brown P, et al. Transmission of Creutzfeldt-Jakob disease via a corneal transplant. J Neurol Neurosurg Psychiatry. 1997;63:388–90.
9. World Health Organization (WHO). WHO infection control guidelines for transmissible spongiform encephalopathies. Report of a WHO consultation, Geneva, Switzerland, 1999 March 23–26. Geneva: WHO; 1999. Available from http://www.who.int/csr/resources/publications/bse/WHO_CDS_CSR_APH_2000_3/en/
10. Masters CL, Harris JO, Gajdusek DC, Gibbs CJ Jr, Bernoulli C, Asher DM. Creutzfeldt-Jakob disease: patterns of worldwide occurrence and the significance of familial and sporadic clustering. Ann Neurol. 1979;5:177–88.
11. World Health Organization (WHO). The revision of the variant Creutzfeldt-Jakob (vCJD) case definition. Report of a WHO consultation. Edinburgh, United Kingdom, 2001 17 May (WHO/CDS/CSR/EPH/2001.5). Geneva: WHO; 2001.
12. Taylor DM. Inactivation of transmissible degenerative encephalopathy agents: a review. Vet J. 2000;159:10–7.
13. S-Juan P, Ward HJ, De Silva R, Knight RS, Will RG. Ophthalmic surgery and Creutzfeldt-Jakob disease. Br J Ophthalmol. 2004;88:446–9.
14. Brenner MH, Curbow B, Javitt JC, Legro MW, Sommer A. Vision change and quality of life in the elderly. Response to cataract surgery and treatment of other chronic ocular conditions. Arch Ophthalmol. 1993;111:680–5.
15. Tamura H, Tsukamoto H, Mukai S, Kato T, Minamoto A, Ohno Y, et al. Improvement in cognitive impairment after cataract surgery in elderly patients. J Cataract Refract Surg. 2004;30:598–602.

Address for correspondence: Masahito Yamada, Department of Neurology and Neurobiology of Aging, Kanazawa University Graduate School of Medical Science, 13-1, Takara-machi, Kanazawa 920-8640, Japan; email: m-yamada@med.kanazawa-u.ac.jp

THE JOURNAL OF BIOLOGICAL CHEMISTRY VOL. 282, NO. 41, pp. 30022–30028, October 12, 2007

Cross-sequence Transmission of Sporadic Creutzfeldt-Jakob Disease Creates a New Prion Strain*

Received for publication, June 5, 2007, and in revised form, August 8, 2007 Published, JBC Papers in Press, August 20, 2007, DOI 10.1074/jbc.M704597200

Atsushi Kobayashi[‡], Masahiro Asano[‡], Shirou Mohri[§], and Tetsuyuki Kitamoto[‡1]

From the [‡]Division of CJD Science and Technology, Department of Prion Research, Tohoku University Graduate School of Medicine, Sendai 980-8575, Japan and [§]Prion Disease Research Center, National Institute of Animal Health, Tsukuba, Ibaraki 305-0856, Japan

The genotype (methionine or valine) at polymorphic codon 129 of the human prion protein (PrP) gene and the type (type 1 or type 2) of abnormal isoform of PrP (PrP^{Sc}) are major determinants of the clinicopathological phenotypes of sporadic Creutzfeldt-Jakob disease (sCJD). Here we found that the transmission of sCJD prions from a patient with valine homozygosity (129V/V) and type 2 PrP^{Sc} (sCJD-VV2 prions) to mice expressing human PrP with methionine homozygosity (129M/M) generated unusual PrP^{Sc} intermediate in size between type 1 and type 2. The intermediate type PrP^{Sc} was seen in all examined dura mater graft-associated CJD cases with 129M/M and plaque-type PrP deposits (p-dCJD). p-dCJD prions and sCJD-VV2 prions exhibited similar transmissibility and neuropathology, and the identical type of PrP^{Sc} when inoculated into PrP-humanized mice with 129M/M or 129V/V. These findings suggest that p-dCJD could be caused by cross-sequence transmission of sCJD-VV2 prions.

Creutzfeldt-Jakob disease (CJD),[2] kuru, scrapie, and bovine spongiform encephalopathy are lethal transmissible neurodegenerative diseases caused by an abnormal isoform of prion protein (PrP^{Sc}), which is converted from the normal cellular isoform (PrP^{C}) (1). The genotype (methionine or valine) at polymorphic codon 129 of the human prion protein (PrP) gene and the type (type 1 or type 2) of PrP^{Sc} in the brain are major determinants of the clinicopathological phenotypes of sporadic CJD (sCJD) (2–5). Type 1 and type 2 PrP^{Sc} are distinguishable according to the size of the proteinase K-resistant core of PrP^{Sc} (PrP^{res}) (21 and 19 kDa, respectively), reflecting differences in the proteinase K cleavage site (at residues 82 and 97, respectively) (2, 3). The genotype at codon 129 also influences the susceptibility to variant CJD (vCJD), iatrogenic CJD, and kuru (6–11). A transmission study using transgenic mice expressing human PrP revealed that the congruency of the genotype at codon 129 between the inoculum and the inoculated transgenic mice determines the susceptibility to sCJD prions (12). Transmission of sCJD prions to mice with an incongruent genotype (referred to as cross-sequence transmission) results in a relatively long incubation period.

The potential for cross-sequence transmission should be considered in the iatrogenic transmission of CJD via cadaveric pituitary hormones, dura mater and corneal grafts, or contaminated neurosurgical instruments. More than half of the reported cases of dura mater graft-associated CJD (dCJD) occurred in Japan, where 123 cases have been recognized as of February 2006 (13–16). The dural grafts used in Japan were manufactured by German companies (13–15). In Europe, 28.4% of sCJD patients are valine homozygotes (129V/V) or methionine/valine heterozygotes at codon 129 (129M/V) (5). Meanwhile, the population data show a high prevalence (91.6%) of methionine homozygosity (129M/M) in Japanese people (17). These data raise the possibility that part of the Japanese dCJD cases might have been caused by cross-sequence transmission of sCJD prions. In fact, there are two distinct phenotypes in dCJD, with the majority represented by a non-plaque type of dCJD (np-dCJD) and the minority by a plaque-type dCJD (p-dCJD) (18–21). The clinicopathological features of np-dCJD are similar to those of sCJD with 129M/M and type 1 PrP^{Sc} (sCJD-MM1) (14). In contrast, p-dCJD cases show unique features characterized by (i) the absence or late occurrence of myoclonus and periodic synchronous discharges on electroencephalogram; (ii) a long incubation period after grafting and a clinical course of long duration, and (iii) plaque-type PrP deposits in the brain (18–25). Although we have classified p-dCJD cases into MM1, the clinicopathological features of p-dCJD are quite different from those of sCJD-MM1 or np-dCJD (18–21). The reason for the existence of two distinct phenotypes in dCJD has remained elusive.

To identify the origin of p-dCJD, we inoculated sCJD prions into mice expressing human PrP with either 129M/M or 129V/V. Here we report that cross-sequence transmission of sCJD prions from a patient with 129V/V and type 2 PrP^{Sc}

* This work was supported by the program for Promotion of Fundamental Studies in Health Sciences of Japanese National Institute of Biomedical Innovation (to S. M. and T. K.), a grant from the Ministry of Health, Labor and Welfare of Japan (to A. K., S. M., and T. K.), and a grant-in-aid for scientific research from the Ministry of Education, Culture, Sports, Science and Technology of Japan (to A. K. and T. K.). The costs of publication of this article were defrayed in part by the payment of page charges. This article must therefore be hereby marked "*advertisement*" in accordance with 18 U.S.C. Section 1734 solely to indicate this fact.

[1] To whom correspondence should be addressed: Div. of CJD Science and Technology, Dept. of Prion Research, Tohoku University Graduate School of Medicine, 2-1 Seiryo-machi, Aoba-ku, Sendai 980-8575, Japan. Tel.: 81-22-717-8143; Fax: 81-22-717-8148; E-mail: kitamoto@mail.tains.tohoku.ac.jp.

[2] The abbreviations used are: PrP, prion protein; PrP^{C}, normal cellular isoform of PrP; PrP^{Sc}, abnormal isoform of PrP; PrP^{res}, proteinase K-resistant core of PrP^{Sc}; 129M/M, methionine homozygosity at codon 129 of the human PrP gene; 129V/V, valine homozygosity at codon 129 of the human PrP gene; CJD, Creutzfeldt-Jakob disease; sCJD, sporadic CJD; p-dCJD, plaque-type dura mater graft-associated CJD; np-dCJD, non-plaque type dura mater graft-associated CJD; vCJD, variant CJD; dCJD, dura mater graft-associated CJD.

TABLE 1
Transmission of sCJD prions to humanized mice with 129M/M or 129V/V

Inoculum	Incubation period				
	Ki-Hu129M/M (1×)[a]	Tg+Ki-Hu129M/M (1.2×)	Tg+Ki-Hu129M$_{4R}$/M$_{4R}$ (9.8×)	Ki-Hu129V/V (1×)	Tg+Ki-Hu129V/V (2.1×)
			days ± S.E. (n/n^0)[b]		
sCJD-MM1 H3	467 ± 24 (8/8)	429 ± 6 (6/6)	175 ± 4 (9/9)	542, 648 (2/5)[c]	288 ± 9 (4/4)
sCJD-VV2 AK	ND[d]	723 ± 79 (4/4)	505 ± 14 (5/5)	312 ± 7 (4/4)	183 ± 5 (11/11)

[a] The expression levels of human PrP in the brains.
[b] n, number of diseased animals; n^0, number of inoculated animals.
[c] Three animals died of causes other than prion disease.
[d] ND, not done.

(sCJD-VV2 prions) caused phenotypes similar to those of p-dCJD.

EXPERIMENTAL PROCEDURES

Production of Knock-in Mice and Transgenic Mice—The production of knock-in mice expressing human PrP with 129M/M (Ki-Hu129M/M) and Ki-Hu129V/V mice has been reported previously (8). Knock-in mice expressing human PrP with 129M/M and four octapeptide repeats (Ki-Hu129M$_{4R}$/M$_{4R}$), transgenic mice expressing human PrP with 129M and four octapeptide repeats (Tg-Hu129M$_{4R}$), and Tg-Hu129M mice were generated as described (26, 27). To evaluate the effect of overexpression of the PrP gene, Ki-Hu129M$_{4R}$/M$_{4R}$, Ki-Hu129M/M, and Ki-Hu129V/V mice were crossed with Tg-Hu129M$_{4R}$, Tg-Hu129M, or Tg-Hu129V mice (8). The expression levels of human PrP in the brains from Tg+Ki-Hu129M$_{4R}$/M$_{4R}$, Tg+Ki-Hu129M/M, and Tg+Ki-Hu129V/V mice were 9.8×, 1.2×, and 2.1×, respectively, the levels observed in Ki-Hu129M/M or Ki-Hu129V/V mice.

Human Brain Inocula—Brain tissues were obtained at autopsy from CJD patients after receiving informed consent for research use. The diagnosis of CJD and the type of PrP^{Sc} were confirmed by neuropathological examination, PrP^{Sc} immunohistochemistry, and Western blotting as described (28, 29). The genotype and the absence of mutations in the coding region of the PrP gene were determined by sequence analysis (30).

Transmission Experiments—Human brain homogenates (10%) and mouse brain homogenates (10%) were prepared as described (27). Transmission studies were performed using 20 μl of the homogenates for intracerebral inoculation or 50 μl for intraperitoneal inoculation (8, 29). Intracerebrally inoculated mice were sacrificed after the onset of disease, and their brains were immediately frozen or fixed in 10% buffered formalin. Intraperitoneally inoculated mice were sacrificed at 75 days post-inoculation, and their spleens were immediately frozen or formalin-fixed.

Immunohistochemistry—Formalin-fixed mouse brains and spleens were treated with 60% formic acid for 1 h to inactivate the infectivity and embedded in paraffin. Tissue sections were pretreated by hydrolytic autoclaving before PrP immunohistochemistry (28). The PrP-N antiserum was used as the primary antibody (31). Goat anti-rabbit immunoglobulins polyclonal antibody labeled with the peroxidase-conjugated dextran polymer, EnVision+ (DakoCytomation) were used as the secondary antibody.

Western Blotting—PrP^{Sc} was extracted from human brains or mouse brains and spleens with collagenase treatment as described (32) with some modifications. For deglycosylation of PrP, samples were treated with PNGase F (New England Biolabs). Samples were subjected to 13.5% SDS-PAGE and Western blotting as described (8). The 3F4 monoclonal antibody (Signet Laboratories) and the ChW antiserum (8) were used as the primary antibodies. Anti-mouse EnVision+ and anti-rabbit EnVision+ were used as the secondary antibodies.

Statistical Analysis—Incubation times are expressed as mean ± S.E.

RESULTS

Transmission of sCJD Prions to PrP-humanized Mice with 129M/M or 129V/V—To investigate whether strain-dependent traits of sCJD prions can be inherited through cross-sequence transmission, we performed intracerebral inoculation of a brain homogenate from a sCJD-MM1 patient (H3) or that from a sCJD-VV2 patient (AK) into PrP humanized mice with the 129M/M or 129V/V genotype. For sCJD-MM1 prions, the incubation times of Ki-Hu129V/V mice were 542 and 648 days (number of diseased animals/number of inoculated animals = 2/5), which were longer than those of Ki-Hu129M/M mice (467 ± 24 days, 8/8) (Table 1). For sCJD-VV2 prions, the mean incubation time of Tg+Ki-Hu129M/M mice was 723 ± 79 days (4/4), which was longer than that of Ki-Hu129V/V mice (312 ± 7 days, 4/4). Immunohistochemical analysis showed diffuse synaptic-type PrP deposits in the brains from both Tg+Ki-Hu129M/M and Tg+Ki-Hu129V/V mice inoculated with sCJD-MM1 prions (Fig. 1*A*). In contrast, Tg+Ki-Hu129V/V mice inoculated with sCJD-VV2 prions showed small plaque-type PrP deposits in the cerebral white matter and granular to diffuse synaptic-type deposits in the gray matter. The plaque-type PrP deposits were more prominent in the brains from Tg+Ki-Hu129M/M mice inoculated with sCJD-VV2 prions, in which larger plaque-type PrP deposits spread throughout the cerebral gray matter and thalamus rather than the white matter. Western blot analysis revealed that the size of PrP^{res} in the brains was maintained after cross-sequence transmission of sCJD-MM1 prions but not sCJD-VV2 prions (Fig. 1, *B* and *C*). Tg+Ki-Hu129V/V mice inoculated with sCJD-MM1 prions produced type 1 PrP^{res} (hereafter denoted as VV[*MM1*]1 PrP^{res}:host genotype[*inoculated prions*]type of generated PrP^{res}), which were identical in size to MM[*MM1*]1 PrP^{res} from Tg+Ki-Hu129M/M mice.

However, Tg+Ki-Hu129M/M mice inoculated with sCJD-VV2 prions produced unusual PrP^{res} that were larger than VV[*VV2*]2 PrP^{res} from Tg+Ki-Hu129V/V mice but smaller than MM[*MM1*]1 or VV[*MM1*]1 PrP^{res}. We designated this intermediate-sized PrP^{res} as MM[*VV2*]2^{Sh+}, PrP^{res} with an upward size shift (Sh+) from the inoculated type 2 template. The shift in the size of PrP^{res} and the prominent plaque formation in Tg+Ki-Hu129M/M mice indicated that the strain-dependent traits of sCJD-VV2 prions were modified through cross-sequence transmission.

Intermediate Type PrP^{res} in Human p-dCJD Cases—Tg+Ki-Hu129M/M mice inoculated with sCJD-VV2 prions showed plaque-type PrP deposits in the brains despite their 129M/M genotype. CJD patients with the 129M/M genotype and plaque-type PrP deposits have been mainly recognized in vCJD and p-dCJD. To date, we have classified vCJD cases into MM2B and p-dCJD cases into MM1. However, there has been an exceptional case of p-dCJD that showed the accumulation of PrP^{res} intermediate in size between type 1 and type 2 (20). The occurrence of plaque-type PrP deposits and MM[*VV2*]2^{Sh+} PrP^{res} in Tg+Ki-Hu129M/M mice inoculated with sCJD-VV2 prions raised the possibility that p-dCJD could be caused by cross-sequence transmission of sCJD-VV2 prions. To address this possibility, we re-examined carefully the size of PrP^{res} in the brains from three p-dCJD patients. Western blot analysis showed that the size of PrP^{res} from p-dCJD cases was smaller than that of MM1 PrP^{res} from sCJD-MM1 or np-dCJD cases (Fig. 2, *A* and *B*). Therefore, it appeared that the intermediate type PrP^{res} reported by Kretzschmar and colleagues (20) is not rare but rather a common form in human p-dCJD cases. We designated this intermediate type PrP^{res} observed in p-dCJD cases as MMi PrP^{res}.

Transmission of p-dCJD Prions to PrP-humanized Mice with 129M/M or 129V/V—To investigate the transmissibility of p-dCJD prions, we performed intracerebral inoculation of brain homogenates from p-dCJD patients (KR, KD, TV) into PrP-humanized mice with the 129M/M or 129V/V genotype. We had already established Ki-Hu129M_{4R}/M_{4R} mice expressing human PrP with 129M/M and four octapeptide repeats before we produced Ki-Hu129M/M mice expressing human PrP with five octapeptide repeats. The four or five octapeptide repeats of human PrP are polymorphisms unassociated with CJD (33). For sCJD-MM1 prions, these Ki-Hu129M_{4R}/M_{4R} mice showed long incubation times of >600 days in our preliminary experiment (data not shown). Therefore, they were crossed with Tg-Hu129M_{4R} mice to overexpress the human PrP gene. Because these Tg+Ki-Hu129M_{4R}/M_{4R} mice were highly susceptible to

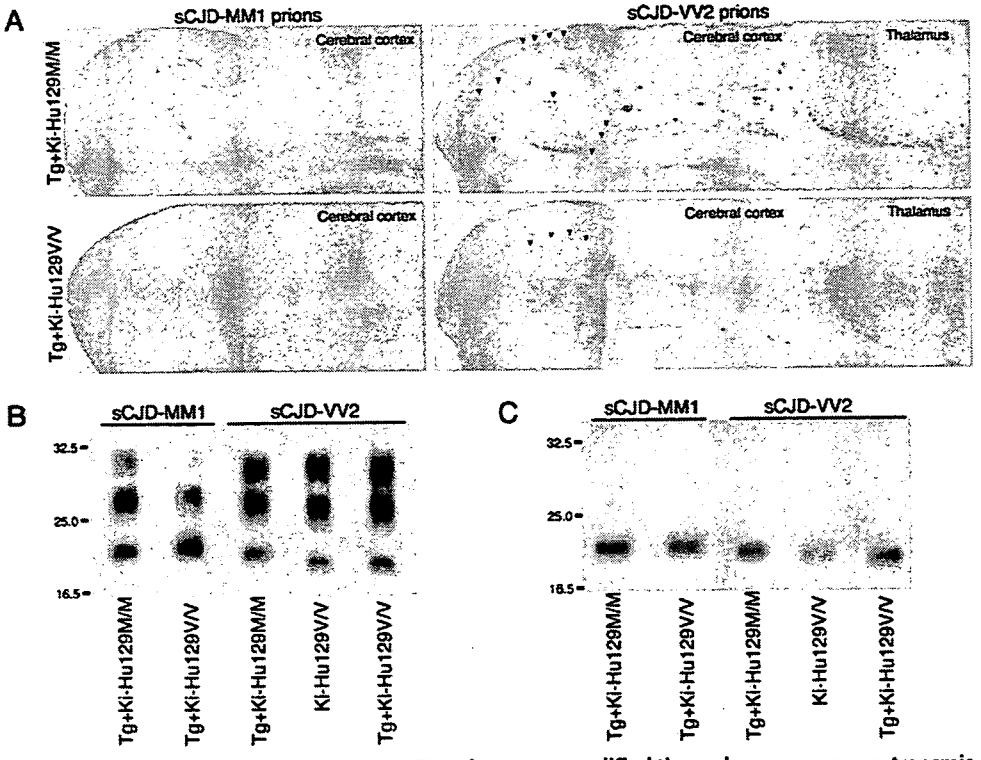

FIGURE 1. **Strain-dependent traits of sCJD-VV2 prions were modified through cross-sequence transmission.** *A*, immunohistochemical analysis of the brains from Tg+Ki-Hu129M/M mice inoculated with sCJD-VV2 prions showed prominent plaque-type PrP deposits (*arrowheads*) throughout the cerebral gray matter and thalamus. In the brains from Tg+Ki-Hu129V/V mice inoculated with sCJD-VV2 prions, plaque-type PrP deposits were restricted to within the white matter. *B*, Western blot analysis of the brains from PrP-humanized mice after proteinase K digestion. *C*, proteinase K-digested samples were treated with PNGase F for deglycosylation of PrP^{res}. Tg+Ki-Hu129M/M mice inoculated with sCJD-VV2 prions produced unusual PrP^{res} intermediate in size between type 1 and type 2 (designated as MM[*VV2*]2^{Sh+} PrP^{res}:host genotype[*inoculated prions*]type of generated PrP^{res}).

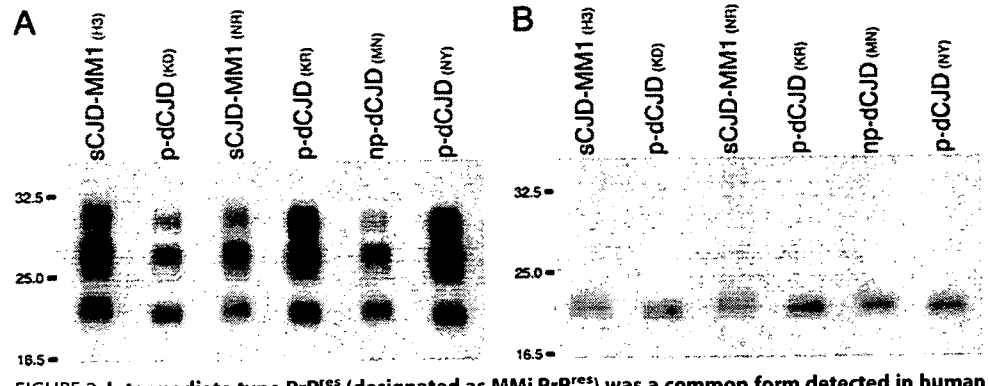

FIGURE 2. **Intermediate type PrP^{res} (designated as MMi PrP^{res}) was a common form detected in human p-dCJD cases.** *A*, Western blot analysis of the brains from dCJD patients or those from sCJD-MM1 patients after proteinase K digestion. *B*, for deglycosylation of PrP^{res}, proteinase K-digested samples were treated with PNGase F. PrP^{res} in the brains from p-dCJD patients were smaller than MM1 PrP^{res} from sCJD-MM1 or np-dCJD cases.

TABLE 2
Transmission of p-dCJD prions or sCJD-VV2 prions to humanized mice with 129M/M or 129V/V

Inoculum	Genotype	Incubation period	
		Tg+Ki-Hu129M$_{4R}$/M$_{4R}$	Ki-Hu129V/V
		days ± S.E. (n/n^0)[a]	
p-dCJD			
KR	129M/M	420 ± 10 (5/5)	259 ± 6 (6/6)
KD	129M/M	398 ± 10 (5/5)	304 ± 13 (6/6)
TV	129M/M	584 ± 65 (5/5)	ND[b]
sCJD-VV2			
AK	129V/V	505 ± 14 (5/5)	312 ± 7 (4/4)

[a] *n*, number of diseased animals; n^0, number of inoculated animals.
[b] ND, not done.

sCJD-MM1 prions (175 ± 4 days, 9/9) (Table 1), we used them as PrP-humanized mice with the 129M/M genotype in this experiment at first. All of Tg+Ki-Hu129M$_{4R}$/M$_{4R}$ and Ki-Hu129V/V mice inoculated with p-dCJD prions developed disease (Table 2). The mean incubation times of Tg+Ki-Hu129M$_{4R}$/M$_{4R}$ mice were 398 ± 10, 420 ± 10, and 584 ± 65 days. Though the expression level of human PrP in Tg+Ki-Hu129M$_{4R}$/M$_{4R}$ mice was 9.8-fold higher than that of Ki-Hu129V/V mice, the mean incubation times of Tg+Ki-Hu129M$_{4R}$/M$_{4R}$ mice were longer than those of Ki-Hu129V/V mice (259 ± 6 and 304 ± 13 days). For np-dCJD, the mean incubation times of Tg+Ki-Hu129M$_{4R}$/M$_{4R}$ mice were 161 ± 5 (5/5) and 208 ± 2 days (5/5). Immunohistochemical analysis of the brains from Tg+Ki-Hu129M$_{4R}$/M$_{4R}$ mice inoculated with p-dCJD prions showed a few plaque-type PrP deposits similar to those in Tg+Ki-Hu129M$_{4R}$/M$_{4R}$ mice inoculated with sCJD-VV2 prions (Fig. 3*A*). Ki-Hu129V/V mice inoculated with p-dCJD prions showed small plaque-type PrP deposits in the cerebral white matter and granular to diffuse synaptic-type deposits in the gray matter similar to those in Ki-Hu129V/V mice inoculated with sCJD-VV2 prions. There was no plaque-type PrP deposits in the brains from Tg+Ki-Hu129M$_{4R}$/M$_{4R}$ mice inoculated with np-dCJD prions (Fig. 3*B*). Western blot analysis revealed that Tg+Ki-Hu129M$_{4R}$/M$_{4R}$ mice inoculated with p-dCJD prions produced the intermediate type PrP^{res} (M$_{4R}$M$_{4R}$[*MMi*]i PrP^{res}), which were identical in size to M$_{4R}$M$_{4R}$[*VV2*]2^{Sh+} PrP^{res} (Fig. 3, *C* and *D*). Furthermore, Ki-Hu129V/V mice inoculated with p-dCJD prions produced type 2 PrP^{res} (VV[*MMi*]2 PrP^{res}), which were identical in size to VV[*VV2*]2 PrP^{res}. Thus, p-dCJD prions and sCJD-VV2 prions were similar in the transmissibility, the patterns of PrP deposition, and the size of PrP^{res} (the intermediate type in Tg+Ki-Hu129M$_{4R}$/M$_{4R}$ or type 2 in Ki-Hu129V/V) in PrP-humanized mice.

On the basis of the following facts, we considered that the number of octapeptide repeats of PrP did not affect the size of PrP^{res}. Tg+Ki-Hu129M4R/M4R mice inoculated with sCJD-MM1 prions produced M$_{4R}$M$_{4R}$[*MM1*]1 PrP^{res} identical in size to MM[*MM1*]1 PrP^{res} from Ki-Hu129M/M mice (Fig. 3*E*). Furthermore, Tg+Ki-Hu129M$_{4R}$/M$_{4R}$ mice inoculated with sCJD-VV2 prions produced M$_{4R}$M$_{4R}$[*VV2*]2^{Sh+} PrP^{res} identical in size to MM[*VV2*]2^{Sh+} PrP^{res} from Tg+Ki-Hu129M/M mice (Fig. 3*E*).

We inoculated intracerebrally a brain homogenate from a p-dCJD patient (KD) into Ki-Hu129M/M mice besides Tg+Ki-Hu129M$_{4R}$/M$_{4R}$ mice. The mean incubation time of these Ki-Hu129M/M mice was 500 ± 59 days (4/4). These mice produced MM[*MMi*]i PrP^{res} identical in size to M$_{4R}$M$_{4R}$[*MMi*]i PrP^{res} from Tg+Ki-Hu129M$_{4R}$/M$_{4R}$ mice (Fig. 3*F*).

Intraperitoneal Transmission of p-dCJD Prions or sCJD-VV2 Prions to PrP-humanized Mice with 129M/M or 129V/V—To confirm the similarity in the transmissibility between p-dCJD prions and sCJD-VV2 prions, we performed intraperitoneal inoculation of the brain homogenate from a p-dCJD patient (KD) or that from a sCJD-VV2 patient (AK) into PrP-humanized mice as described previously (27). Immunohistochemical analysis of the spleens at 75 days post-inoculation revealed that Ki-Hu129V/V mice were more susceptible to p-dCJD prions than Ki-Hu129M/M mice (Fig. 4*A*). Similarly, Ki-Hu129V/V mice were more susceptible to sCJD-VV2 prions than Ki-Hu129M/M mice. In contrast, Ki-Hu129V/V mice intraperitoneally inoculated with sCJD-MM1 prions showed no obvious PrP deposition in the spleen (0/9). Therefore, we confirmed that p-dCJD prions and sCJD-VV2 prions exhibited similar transmissibility to PrP-humanized mice even in peripheral infection. In addition, Ki-Hu129M/M mice intraperitoneally inoculated with sCJD-VV2 prions produced MM[*VV2*]2^{Sh+} PrP^{res} in the spleen (Fig. 4*B*). Meanwhile, Ki-Hu129V/V mice intraperitoneally inoculated with sCJD-VV2 prions produced VV[*VV2*]2 PrP^{res}. Thus, we confirmed the shift of the PrP^{res} size also in the spleens.

Because cross-sequence transmission of sCJD-VV2 prions to Tg+Ki-Hu129M/M mice caused phenotypes similar to those of p-dCJD, we also examined the transmissibility of Tg+Ki-Hu129M/M mouse-passaged sCJD-VV2 prions (designated as MM[*VV2*]2^{Sh+} prions). We performed intraperitoneal inoculation of the brain homogenate from a Tg+Ki-Hu129M/M mouse that succumbed to sCJD-VV2 prions into PrP-humanized mice. All (11/11) of Ki-Hu129V/V mice inoculated with MM[*VV2*]2^{Sh+} prions showed PrP deposition in the spleen despite cross-sequence transmission. Western blot analysis of the spleens revealed that Ki-Hu129M/M mice produced type 2^{Sh+} PrP^{res} (MM[*MM[VV2]2^{Sh+}*]2^{Sh+} PrP^{res}) identical in size to MM[*VV2*]2^{Sh+} PrP^{res}. Meanwhile, Ki-Hu129V/V mice produced type 2 PrP^{res} (VV[*MM[VV2]2^{Sh+}*]2 PrP^{res}) identical in size to VV[*VV2*]2 PrP^{res}(Fig. 4*B*).

DISCUSSION

Our data comprised of four major findings. First, transmission of sCJD-VV2 prions to Tg+Ki-Hu129M/M mice generated unusual PrP^{res} (MM[*VV2*]2^{Sh+} PrP^{res}) intermediate in size between type 1 and type 2. Second, the intermediate type MMi PrP^{res} was seen in all examined p-dCJD cases. Third, Ki-Hu129V/V mice inoculated with p-dCJD prions showed short incubation times and the accumulation of type 2 PrP^{res} with a downward size shift from the intermediate type template. Finally, Ki-Hu129V/V mice intraperitoneally inoculated with MM[*VV2*]2^{Sh+} prions showed high susceptibility and the accumulation of type 2 PrP^{res} with a downward size shift from type 2^{Sh+} template. These findings suggest that p-dCJD could be caused by transmission of sCJD-VV2 prions to individuals with the 129M/M genotype (cross-sequence transmission).

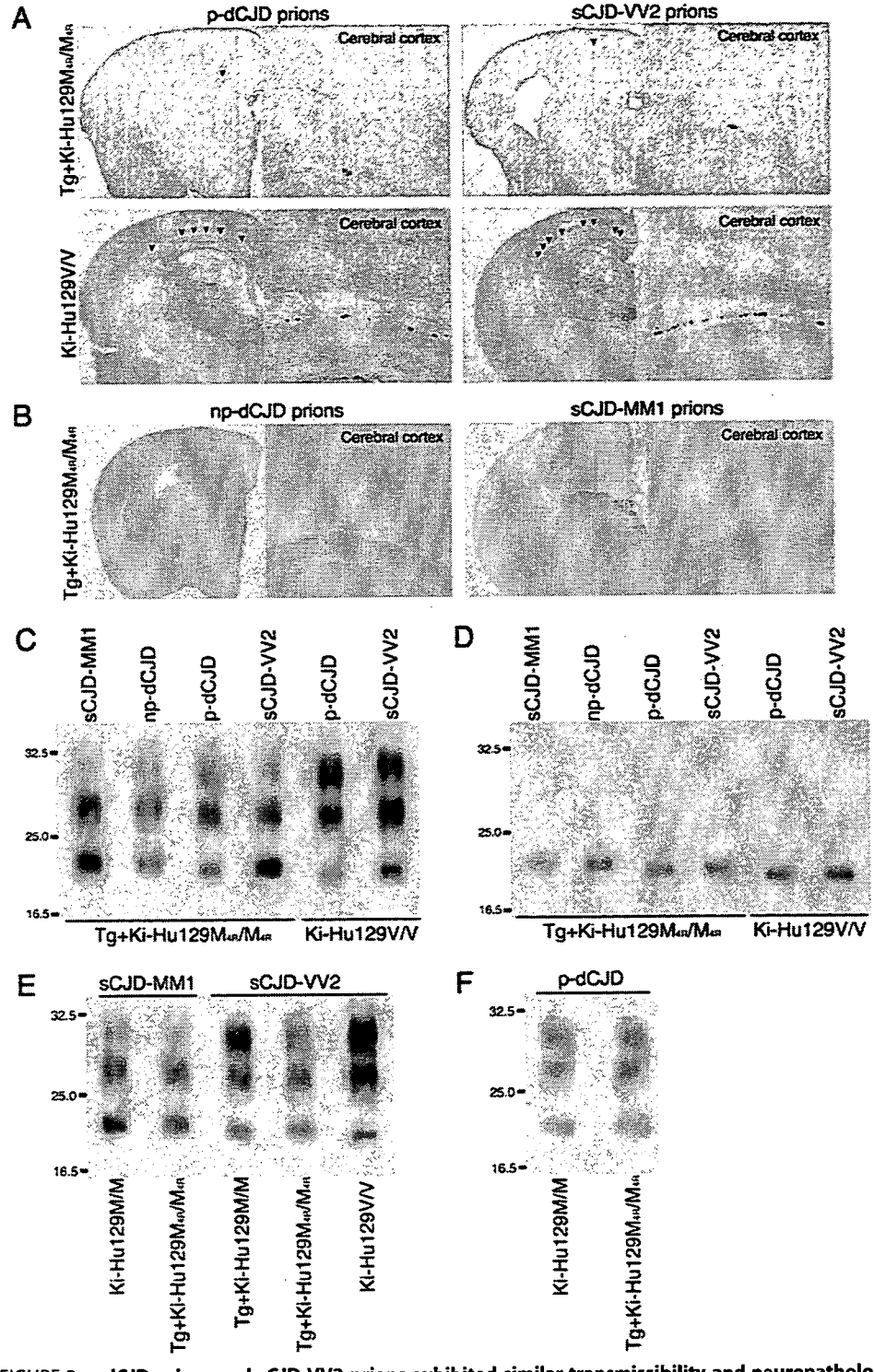

FIGURE 3. **p-dCJD prions and sCJD-VV2 prions exhibited similar transmissibility and neuropathology and identically sized PrP^{res} in PrP-humanized mice.** *A*, immunohistochemical analysis of the brains from Tg+Ki-Hu129M_{4R}/M_{4R} mice inoculated with p-dCJD prions or sCJD-VV2 prions showed a few plaque-type PrP deposits (*arrowheads*). Ki-Hu129V/V mice inoculated with p-dCJD prions or sCJD-VV2 prions showed small plaque-type PrP deposits in the cerebral white matter and synaptic-type deposits in the gray matter. *B*, diffuse synaptic-type PrP deposits in the brains from Tg+Ki-Hu129M_{4R}/M_{4R} mice inoculated with np-dCJD prions or sCJD-MM1 prions. There was no plaque-type PrP deposits. *C*, Western blot analysis of the brains from PrP-humanized mice after proteinase K digestion. *D*, for deglycosylation of PrP^{res}, proteinase K-digested samples were treated with PNGase F. Tg+Ki-Hu129M_{4R}/M_{4R} mice inoculated with p-dCJD prions or sCJD-VV2 prions produced the intermediate type PrP^{res}. Meanwhile, Ki-Hu129V/V mice inoculated with p-dCJD prions or sCJD-VV2 prions produced type 2 PrP^{res}. *E*, Tg+Ki-Hu129M_{4R}/M_{4R} mice inoculated with sCJD-MM1 prions produced M_{4R}/M_{4R}[*MM1*]1 PrP^{res} identical in size to MM[*MM1*]1 PrP^{res} from Ki-Hu129M/M mice. Tg+Ki-Hu129M_{4R}/M_{4R} mice inoculated with sCJD-VV2 prions produced M_{4R}/M_{4R}[*VV2*]2^{Sh+} PrP^{res} identical in size to MM[*VV2*]2^{Sh+} PrP^{res} from Tg+Ki-Hu129M/M mice. *F*, Ki-Hu129M/M mice inoculated with p-dCJD prions produced MM[*MM1*]i PrP^{res} identical in size to M_{4R}/M_{4R}[*MM1*]i PrP^{res} from Tg+Ki-Hu129M_{4R}/M_{4R} mice.

Our results clearly demonstrate that p-dCJD prions and np-dCJD prions are distinct strains. On careful examination, the intermediate type PrP^{res} was found to be a common form in p-dCJD cases. Moreover, the characteristic features of p-dCJD including the intermediate type PrP^{res}, the long incubation period, and plaque-type PrP deposits in the brain were maintained after transmission to PrP-humanized mice with 129M/M. Meanwhile, the humanized mice with 129M/M inoculated with np-dCJD prions showed type 1 PrP^{res}, a short incubation period, and synaptic-type PrP deposits in the brain. These results demonstrate that p-dCJD and np-dCJD are distinct subtypes of d-CJD caused by distinct prion strains. The long incubation times of the mice inoculated with p-dCJD prions suggest the frightening possibility that the numbers of p-dCJD patients may increase in the future.

sCJD cases with the 129M/V genotype and type 2 PrP^{Sc} (sCJD-MV2) and sCJD-VV2 cases account for 25% of the total sCJD cases and show the characteristic neuropathological changes highlighted by plaque-type PrP deposits (5). To date, some similarities among sCJD-MV2, sCJD-VV2, and p-dCJD have been described in clinicopathological, biochemical, and transmission studies (18–21, 29). Although the results of the present study show that cross-sequence transmission of sCJD-VV2 prions can cause phenotypes similar to those of p-dCJD, further studies are needed to clarify whether sCJD-MV2 prions can cause a p-dCJD like phenotype in humanized mice with 129M/M.

Besides p-dCJD, a few iatrogenic CJD cases with the 129M/M genotype and plaque-type PrP deposits in the brain have been reported in human growth hormone-related CJD (34, 35). The present results lead us to surmise that the human growth hormone-related CJD cases with 129M/M and plaque-type PrP deposits might be caused by the cross-sequence transmission of sCJD-VV2 prions.

A

Inoculum	Genotype	Susceptibility[a] (n/n^{o})[b] Ki-Hu129M/M	Ki-Hu129V/V
p-dCJD	KD 129M/M	0/6	5/6
sCJD-VV2	AK 129V/V	3/10	10/12

[a] Positives were confirmed by immunohistochemical analysis of the spleens.
[b] n, number of animals with positive labeling of abnormal PrP in the spleens; n^{o}, number of inoculated animals.

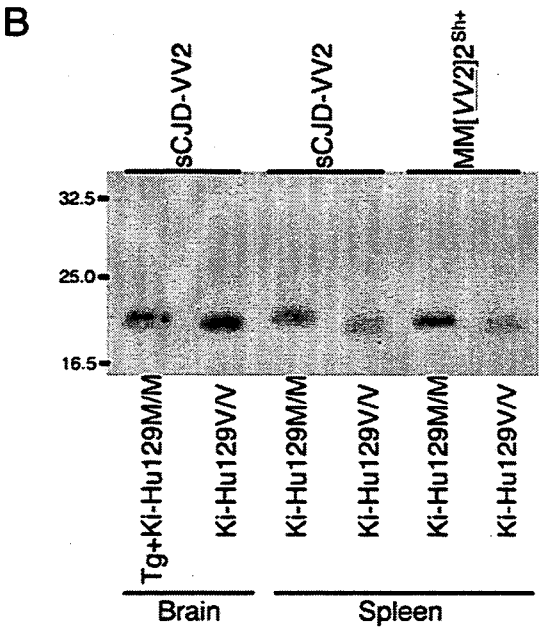

FIGURE 4. **Intraperitoneal transmission of p-dCJD prions, sCJD-VV2 prions, or Tg+Ki-Hu129M/M mouse-passaged sCJD-VV2 prions (designated as MM[*VV2*]2^{Sh+} prions) to PrP-humanized mice.** *A*, Ki-Hu129V/V mice were highly susceptible to p-dCJD prions and sCJD-VV2 prions even in peripheral infection. *B*, Western blot analysis of the spleens after proteinase K digestion and PNGase F treatment. Ki-Hu129M/M mice intraperitoneally inoculated with sCJD-VV2 prions produced MM[*VV2*]2^{Sh+} PrP^{res} identical in size to those seen in the brain after intracerebral inoculation. Ki-Hu129M/M mice inoculated with MM[*VV2*]2^{Sh+} prions produced type 2^{Sh+} PrP^{res} identical in size to MM[*VV2*]2^{Sh+} PrP^{res}. Meanwhile, Ki-Hu129V/V mice inoculated with MM[*VV2*]2^{Sh+} prions produced type 2 PrP^{res}.

Through cross-sequence transmission, sCJD-VV2 prions acquired new conformational properties as reflected by the upward shift of the size of PrP^{res}. A similar shift of the PrP^{res} size through cross-sequence transmission has been reported in mice inoculated with vCJD prions (29, 36) or hamster scrapie strain Sc237 (37, 38). Moreover, the altered size of mouse-passaged Sc237 PrP^{res} reverts to those of hamster-passaged Sc237 PrP^{res} through transmission to hamsters (37). In accordance with these findings, the intermediate type PrP^{res} reverted to type 2 when MM[*VV2*]2^{Sh+} prions or p-dCJD prions were transmitted to the humanized mice with 129V/V in this study. The most plausible explanation for these findings is that adaptation to the new host PrP^{C} and/or selection of a PrP^{Sc} subpopulation from the whole heterogeneous population result in the emergence of a new prion strain with altered conformational properties, and that the emerging prion strain retains the memory of the parental prions within its conformational properties and/or its PrP^{Sc} subpopulation. Therefore, if the emerging prion strain is transmitted to the original host, the parental prions may re-emerge and become dominant.

The above concept is supported by the "traceback" phenomenon (8), *e.g.* knock-in mice and transgenic mice expressing bovine PrP are highly susceptible to vCJD prions as well as bovine spongiform encephalopathy prions (8, 39). Consistent with a report using transgenic mice expressing human PrP with 129M or 129V (12), the humanized mice with 129V/V in our study were more susceptible to sCJD-VV2 prions than the humanized mice with 129M/M. Furthermore, the humanized mice with 129V/V showed high susceptibility to MM[*VV2*]2^{Sh+} prions and p-dCJD prions despite cross-sequence transmission. These phenomena can be explained as follows. Because MM[*VV2*]2^{Sh+} prions and p-dCJD prions retained the memory of the parental sCJD-VV2 prions, the humanized mice with 129V/V were highly susceptible to these prions as well as sCJD-VV2 prions. Our results demonstrate that traceback studies can be a powerful tool to identify the origin of prions.

In this study, the strain-dependent traits of sCJD-MM1 prions were inherited through cross-sequence transmission without any modification. The humanized mice with 129V/V produced type 1 PrP^{res} after inoculation with sCJD-MM1 prions. Because sCJD-VV1 cases are extremely rare (at most 1–2% of the total number of sCJD cases) and characterized by early onset (mean age at onset, 39.3 years) (5), our results raise the possibility that CJD cases classified as VV1 may include cases caused by iatrogenic transmission of sCJD-MM1 prions or food-borne infection by type 1 prions from animals, *e.g.* chronic wasting disease prions in cervid. In fact, two CJD-VV1 patients who hunted deer or consumed venison have been reported (40, 41). The results of the present study emphasize the need for traceback studies and careful re-examination of the biochemical properties of sCJD-VV1 prions.

In conclusion, cross-sequence transmission of sCJD-VV2 prions generates a new prion strain with altered conformational properties and disease phenotypes as p-dCJD prions. Furthermore, the newly generated prions have unique transmissibility including the traceback phenomenon. In the future, if atypical prion strains emerge through cross-sequence transmission, especially from animals, traceback studies will enable us to identify the origin of the prions.

Acknowledgments—We thank H. Kudo and K. Abe for technical assistance and R.-W. Shin and B. Bell for critical review of the manuscript.

REFERENCES

1. Prusiner, S. B., Scott, M. R., DeArmond, J. P., and Cohen, F. E. (1998) *Cell* **93,** 337–348
2. Parchi, P., Castellani, R., Capellari, S., Ghetti, B., Young, K., Chen, S. G., Farlow, M., Dickson, D. W., Sima, A. A. F., Trojanowski, J. Q., Petersen, R. B., and Gambetti, P. (1996) *Ann. Neurol.* **39,** 767–778
3. Parchi, P., Zou, W., Wang, W., Brown, P., Capellari, S., Ghetti, B., Kopp, N., Schulz-Schaeffer, W. J., Kretzschmar, H. A., Head, M. W., Ironside, J. W., Gambetti, P., and Chen, S. G. (2000) *Proc. Natl. Acad. Sci. U. S. A.* **97,** 10168–10172
4. Parchi, P., Capellari, S., Chen, S. G., Petersen, R. B., Gambetti, P., Kopp, N., Brown, P., Kitamoto, T., Tateishi, J., Giese, A., and Kretzschmar, H. (1997) *Nature* **386,** 232–234

5. Parchi, P., Giese, A., Capellari, S., Brown, P., Schulz-Schaeffer, W., Windl, O., Zerr, I., Budka, H., Kopp, N., Piccardo, P., Poser, S., Rojiani, A., Streichemberger, N., Julien, J., Vital, C., Ghetti, B., Gambetti, P., and Kretzschmar, H. (1999) *Ann. Neurol.* **46,** 224–233
6. Zeidler, M., Stewart, G., Cousens, S. N., Estibeiro, K., and Will, R. G. (1997) *Lancet* **350,** 668
7. Wadsworth, J. D. F., Asante, E. A., Desbruslais, M., Linehan, J. M., Joiner, S., Gowland, I., Welch, J., Stone, L., Lloyd, S. E., Hill, A. F., Brandner, S., and Collinge, J. (2004) *Science* **306,** 1793–1796
8. Asano, M., Mohri, S., Ironside, J. W., Ito, M., Tamaoki, N., and Kitamoto, T. (2006) *Biochem. Biophys. Res. Commun.* **342,** 293–299
9. Collinge, J., Palmer, M. S., and Dryden, A. J. (1991) *Lancet* **337,** 1441–1442
10. Deslys, J. P., Marce, D., and Dormont, D. (1994) *J. Gen. Virol.* **75,** 23–27
11. Lee, H. S., Brown, P., Cervenáková, L., Garruto, R. M., Alpers, M. P., Gajdusek, D. C., and Goldfarb, L. G. (2001) *J. Infect. Dis.* **183,** 192–196
12. Korth, C., Kaneko, K., Groth, D., Heye, N., Telling, G., Mastrianni, J., Parchi, P., Gambetti, P., Will, R., Ironside, J., Heinrich, C., Tremblay, P., DeArmond, S. J., and Prusiner, S. B. (2003) *Proc. Natl. Acad. Sci. U. S. A.* **100,** 4784–4789
13. Brown, P., Preece, M., Brandel, J. P., Sato, T., McShane, L., Zerr, I., Fletcher, A., Will, R. G., Pocchiari, M., Cashman, N. R., d'Aignaux, J. H., Cervenáková, L., Fradkin, J., Schonberger, L. B., and Collins, S. J. (2000) *Neurology* **55,** 1075–1081
14. Hoshi, K., Yoshino, H., Urata, J., Nakamura, Y., Yanagawa, H., and Sato, T. (2000) *Neurology* **55,** 718–721
15. Nakamura, Y., Watanabe, M., Nagoshi, K., Kitamoto, T., Sato, T., Yamada, M., Mizusawa, H., Maddox, R., Sejvar, J., Belay, E., and Schonberger, L. B. (2003) *MMWR. Morb. Mortal. Wkly. Rep.* **52,** 1179–1181
16. Brown, P., Brandel, J. P., Preese, M., and Sato, T. (2006) *Neurology* **67,** 389–393
17. Doh-ura, K., Kitamoto, T., Sakaki, Y., and Tateishi, J. (1991) *Nature* **353,** 801–802
18. Shimizu, S., Hoshi, K., Muramoto, T., Homma, M., Ironside, J. W., Kuzuhara, S., Sato, T., Yamamoto, T., and Kitamoto, T. (1999) *Arch. Neurol.* **56,** 357–362
19. Mochizuki, Y., Mizutani, T., Tajiri, N., Oinuma, T., Nemoto, N., Kakimi, S., and Kitamoto, T. (2003) *Neuropathology* **23,** 136–140
20. Kretzschmar, H. A., Sethi, S., Földvári, Z., Windl, O., Querner, V., Zerr, I., and Poser, S. (2003) *Brain Pathol.* **13,** 245–249
21. Satoh, K., Muramoto, T., Tanaka, T., Kitamoto, N., Ironside, J. W., Nagashima, K., Yamada, M., Sato, T., Mohri, S., and Kitamoto, T. (2003) *J. Gen. Virol.* **84,** 2885–2893
22. Lane, K. L., Brown, P., Howell, D. N., Chain, B. J., Hulette, C. M., Burger, P. C., and DeArmond, S. J. (1994) *Neurosurgery* **34,** 737–740
23. Kopp, N., Streichenberger, N., Deslys, J. P., Laplanche, J. L., and Chazot, G. (1996) *Lancet* **348,** 1239–1240
24. Takashima, S., Tateishi, J., Taguchi, Y., and Inoue, H. (1997) *Lancet* **350,** 865–866
25. Kimura, K., Nonaka, A., Tashiro, H., Yaginuma, M., Shimokawa, R., Okeda, R., and Yamada, M. (2001) *J. Neurol. Neurosurg. Psychiatry* **70,** 696–699
26. Kitamoto, T., Nakamura, K., Nakao, K., Shibuya, S., Shin, R. W., Gondo, Y., Katsuki, M., and Tateishi, J. (1996) *Biochem. Biophys. Res. Commun.* **222,** 742–747
27. Kitamoto, T., Mohri, S., Ironside, J. W., Miyoshi, I., Tanaka, T., Kitamoto, N., Itohara, S., Kasai, N., Katsuki, M., Higuchi, J., Muramoto, T., and Shin, R. W. (2002) *Biochem. Biophys. Res. Commun.* **294,** 280–286
28. Kitamoto, T., Shin, R. W., Doh-ura, K., Tomokane, N., Miyazono, M., Muramoto, T., and Tateishi, J. (1992) *Am. J. Pathol.* **140,** 1285–1294
29. Taguchi, Y., Mohri, S., Ironside, J. W., Muramoto, T., and Kitamoto, T. (2003) *Am. J. Pathol.* **163,** 2585–2593
30. Kitamoto, T., Ohta, M., Doh-ura, K., Hitoshi, S., Terao, Y., and Tateishi, J. (1993) *Biochem. Biophys. Res. Commun.* **191,** 709–714
31. Kitamoto, T., Muramoto, T., Hilbich, C., Beyreuther, K., and Tateishi, J. (1991) *Brain Res.* **545,** 319–321
32. Grathwohl, K. U. D., Horiuchi, M., Ishiguro, N., and Shinagawa, M. (1996) *Arch. Virol.* **141,** 1863–1874
33. Palmer, M. S., Mahal, S. P., Campbell, T. A., Hill, A. F., Sidle, K. C. L., Laplanche, J. L., and Collinge, J. (1993) *Hum. Mol. Genet.* **2,** 541–544
34. Delisle, M. B., Fabre, N., Rochiccioli, P., Doerr-Schott, J., Rumeau, J. L., and Bes, A. (1993) *Rev. Neurol. (Paris)* **149,** 524–527
35. Billette de Villemeur, T., Gelot, A., Deslys, J. P., Dormont, D., Duyckaerts, Ch., Jardin, L., Denni, J., and Robain, O. (1994) *Neuropathol. Appl. Neurobiol.* **20,** 111–117
36. Hill, A. F., Desbruslais, M., Joiner, S., Sidle, K. C. L., Gowland, I., and Collinge, J. (1997) *Nature* **389,** 448–450
37. Hill, A. F., Joiner, S., Linehan, J., Desbruslais, M., Lantos, P. L., and Collinge, J. (2000) *Proc. Natl. Acad. Sci. U. S. A.* **97,** 10248–10253
38. Peretz, D., Williamson, R. A., Legname, G., Matsunaga, Y., Vergara, J., Burton, D. R., DeArmond, S. J., Prusiner, S. B., and Scott, M. R. (2002) *Neuron* **34,** 921–932
39. Scott, M. R., Peretz, D., Nguyen, H. O. B., DeArmond, S. J., and Prusiner, S. B. (2005) *J. Virol.* **79,** 5259–5271
40. Belay, E. D., Gambetti, P., Schonberger, L. B., Parchi, P., Lyon, D. R., Capellari, S., McQuiston, J. H., Bradley, K., Dowdle, G., Crutcher, J. M., and Nichols, C. R. (2001) *Arch. Neurol.* **58,** 1673–1678
41. Belay, E. D., Maddox, R. A., Williams, E. S., Miller, M. W., Gambetti, P., and Schonberger, L. B. (2004) *Emerg. Infect. Dis.* **10,** 977–984

Neuropathology 2007; **27**, 314–323 doi:10.1111/j.1440-1789.2007.00781.x

Original Article

Enhanced Aquaporin-4 immunoreactivity in sporadic Creutzfeldt-Jakob disease

Yasushi Iwasaki,[1] Maya Mimuro,[2] Mari Yoshida,[2] Yoshio Hashizume,[2] Masumi Ito,[1] Tetsuyuki Kitamoto,[3] Yoshihiro Wakayama[4] and Gen Sobue[1]

[1]Department of Neurology, Nagoya University Graduate School of Medicine, Nagoya, [2]Department of Neuropathology, Institute for Medical Science of Aging, Aichi Medical University, Aichi-gun, [3]Division of CJD Science and Technology, Department of Prion Research, Center for Translational and Advanced Animal Research on Human Diseases, Tohoku University Graduate School of Medicine, Sendai, and [4]Department of Neurology, Showa University Fujigaoka Hospital, Yokohama, Japan

Aquaporin-4 (AQP-4) is a water channel protein located on the plasma membrane of astrocytes and is regulated under various conditions. In the present study, a series of brains with sporadic Creutzfeldt-Jakob disease (sCJD) were investigated to determine the possible contribution of AQP-4 in the development of sCJD pathology. Six cases of subacute spongiform encephalopathy (SSE) and four cases of panencephalopathic (PE)-type sCJD were included. Increased AQP-4 immunoreactivity compared to that in controls was observed in all sCJD patients, particularly in the cerebral neocortex and cerebellar cortex. AQP-4 immunoreactivity was present in the cell bodies and processes of protoplasmic astrocytes in SSE and around cell bodies and processes of hypertrophic astrocytes in PE-type sCJD. Analysis of serial sections showed the development of sCJD pathology, particularly in neocortical lesions, as follows: PrP deposition; spongiform change and gliosis; enhanced staining for AQP-4; hypertrophic astrocytosis; and neuronal loss and tissue rarefaction. Strong AQP-4 immunoreactivity was present in burnt-out lesions such as those of status spongiosus. These results indicate that increased AQP-4 expression in sCJD is an early pathologic event and appears to remain until the late disease stage. We suggest that increased expression of AQP-4 is a pathologic feature of sCJD.

Correspondence: Yasushi Iwasaki, MD, Department of Neurology, Nagoya University Graduate School of Medicine, 65 Tsurumai-cho, Showa-ku, Nagoya 466-8550, Japan. Email: iwasaki@sc4.so-net.ne.jp

Received 24 August 2006; accepted 1 October 2006.

Key words: Aquaporin-4, astrocyte, prion protein, spongiform change, sporadic Creutzfeldt-Jakob disease.

INTRODUCTION

Aquaporin (AQP) family members are water channel proteins located on the plasma membrane of cells in various tissues. AQPs regulate the water balance at the interface between different tissues.[1–3] AQP-1, AQP-4 and other AQP subtypes have been identified in the central nervous system.[1] The distribution of AQP-1 is restricted to the choroid plexus,[2] and AQP-4 is present in cells lining the subarachnoid space and ventricles under normal conditions.[3–7] A double-labeling study showed that AQP-4 immunoreactivity was restricted to astrocytes and was localized along the entire cell process, including end feet facing the outer surface of capillaries.[8] Enhanced expression of AQP-4 has consistently been reported in astrocytes in various inflammatory lesions, including those of multiple sclerosis, human immunodeficiency virus encephalitis and progressive multifocal leukoencephalopathy.[8] The distribution of AQP4-positive astrocytes differs according to disease and is not necessarily related to brain edema, indicating other functions of AQP-4 in the human brain.[8]

The neuropathologic hallmarks of sporadic Creutzfeldt-Jakob disease (sCJD) include spongiform change in the neuropil, neuronal loss, intense hypertrophic astrocytosis and abnormal protease-resistant prion protein (PrP) deposition.[9–11] Inflammatory reactions and edema are not generally observed in sCJD.[10] Enhanced expression of AQP-4 in sCJD was first reported by our laboratory[12] and has been recently reported by others.[13] In the present study, we further examined the relation between enhanced expression of AQP-4 and sCJD pathology.

Table 1 Summary of 10 Creutzfeldt-Jakob disease cases

Case	Sex	Age at onset (years)	Age at death (years)	Disease duration (months)	Myoclonus	PSWCs	Brain pathlogy findings	Brain weight (g)	Codon 129	Codon 219	PrP type
1	M	82	82	2	+	+	SSE	1240	Met/Met	Glu/Glu	1
2	F	74	74	2	+	–	SSE	1040	Met/Met	Glu/Glu	1
3	M	59	59	3	+	+	SSE	1520	Met/Met	Glu/Glu	1
4	M	60	60	4	+	+	SSE	1200	Met/Met	Glu/Glu	1
5	M	89	89	4	+	+	SSE	1295	Met/Val	Glu/Glu	1
6	F	82	83	5	+	+	SSE	1110	Met/Met	Glu/Glu	1
7	F	58	59	14	+	+	PE	840	Met/Met	Glu/Glu	1
8	F	63	64	16	+	+	PE	820	Met/Met	Glu/Glu	1
9	M	65	67	20	+	+	PE	700	Met/Met	Glu/Glu	1
10	F	53	58	58	+	+	PE	800	Met/Met	Glu/Glu	1

F, female; Glu, glutamic acid; M, male; Met, methionine; PE, panencephalopathic-type; PSWCs, periodic sharp wave complexes; SSE, subacute spongiform encephalopathy; Val, valine.

MATERIALS AND METHODS

Cerebrum and cerebellum from 10 patients with sCJD (five men, five women) were obtained from the Department of Neuropathology, Institute for Medical Science of Aging, Aichi Medical University, Aichi, Japan. No cases with inflammatory complications, such as pneumonia or sepsis, were included in the present study. Clinical information, arranged in order of disease duration, is listed in Table 1. The average age at onset was 68.5 ± 12.3 years (range, 53–89 years), with an average disease duration of 12.8 ± 17.2 months (range, 2–58 months). Average brain weight was 1056.5 ± 263.5 g (range, 700–1520 g). All patients were Japanese, and none had a family history of prion disease. There was no evidence of iatrogenic etiology due to cadaveric dura transplantation or growth hormone administration. No patient had any other clinical or neuropathologic disorders. All patients exhibited typical neuropathologic features of sCJD, including PrP immunoreactivity, and all fulfilled the criteria for pathologic diagnosis of sCJD.[9] Disease was classified according to cerebral pathology findings as either subacute spongiform encephalopathy (SSE), which results predominantly in damage to the cerebral and cerebellar cortices with relatively well-preserved cerebral white matter, or panencephalopathic (PE)-type sCJD, which results in damage to the cerebral and cerebellar cortices and also in extensive degeneration of the cerebral white matter.[11,14] Two normal control brains were also obtained (from a 40-year-old and a 61-year-old man). Neither case showed any clinical or neuropathologic disorders; both patients died of acute heart failure.

Formalin-fixed, paraffin-embedded blocks, including cerebral cortex and white matter and cerebellar cortex and white matter, were prepared. Eight micrometer-thick sections were deparaffinized, dehydrated and stained. For routine microscopic examination, the sections were treated with hematoxylin and eosin (H&E) stain. AQP-4 immunoreactivity was evaluated with the use of affinity purified polyclonal sheep anti-rat AQP-4 antibody raised against a synthetic peptide (CEKKGKDSSGEVLSSV) homologous to the C-terminal end of the cytoplasmic domain of rat AQP-4.[15,16] The specificity of the polyclonal AQP-4 antibody, which cross-reacts with human AQP-4, has been reported.[16] Sections were incubated with 5 g/mL AQP-4 antibody for 2 h at room temperature and then incubated for 1 h with horseradish peroxidase-conjugated secondary goat anti-sheep antibody (1:1000; Dako, Glostrup, Denmark). Peroxidase labeling was visualized with 3,3'-diaminobenzidine/peroxidase (Wako Pure Chemical Industries, Osaka, Japan). To clarify the relation between AQP-4 immunoreactivity and spongiform change, astrocytosis, neuronal loss and PrP deposition, serial sections were subjected to H&E staining and immunostaining for AQP-4 and either antihuman glial fibrillary acidic protein (GFAP) antibody (1:1000; Dako) or anti-PrP (3F4, 1:200; Dako) antibody. GFAP immunostaining was performed with the labeled streptavidin-biotin method (LSAB Kit, Dako) as described previously.[17] PrP immunostaining was performed with the EnVision amplified method (EnVision Plus Kit, Dako) as described previously.[18]

The degree of AQP-4 immunoreactivity was classified as – (no staining), ± (little staining), + (mild staining), ++ (moderate staining) or +++ (strong staining).

Prion protein gene analysis and Western blot analysis

Genomic DNA was extracted from each frozen sCJD cerebral cortex sample and was used to amplify the open reading frame of the PrP gene by polymerase chain reaction. We searched for PrP gene mutations and polymorphisms at codons 129 and 219 by restriction fragment length polymorphism analysis and by sequencing, as described previously.[11]

Table 2 Neuropathologic findings and aquaporin-4 immunoreactivity

Case	Neuropathologic findings						Aquaporin-4 immunoreactivity				
CJD	Cerebrum		Cerebellum				Cerebrum				
	Neocortex	White matter	Molecular layer	Purkinje neuron layer	Granule cell layer	White matter	Neocortex			White matter	
							Pia mater and subpial zone	Around blood vessels	Parenchyma	Around blood vessels	Parenchyma
1	+	−	+	−	±	−	++	+	++	+	−
2	+	−	+	−	±	−	++	+	+	+	−
3	+	−	+	−	±	−	+++	++	+	+	−
4	+	−	+	−	±	−	+++	++	++	±	−
5	++	−	+	−	+	−	+++	++	+	±	−
6	++	±	++	−	+	−	+++	++	++	+	±
7	+++	++	++	±	++	++	+++	++	++	+	+
8	+++	++	+++	±	++	++	+++	++	++	++	++
9	+++	+++	+++	+	+++	++	+++	++	+++	++	++
10	+++	+++	+++	++	+++	+++	+++	++	+++	+	+++
Control											
N1	−	−	−	−	−	−	+	±	−	±	−
N2	−	−	−	−	−	−	+	±	−	±	−

Neuropathologic findings: +++, severe; ++, moderate; +, mild; ±, few; −, none. Aquaporin-4 immunoreactivity: +++, strong; ++, moderate; +, mild; ±, little: −, no staining. CJD, Creutzfeldt-Jakob disease.

Each frozen sCJD cerebral cortex sample was homogenized, and Western blot analysis of protease K-resistant PrP was performed with PrP monoclonal antibody 3F4, as described previously.[11] Typing of PrP was performed on the basis of the classification system proposed by Parchi *et al.*[19]

RESULTS

Prion protein gene analysis and Western blot analysis

PrP gene analysis showed no mutation in any of the sCJD patients. Nine patients showed methionine homozygosity at polymorphic codon 129, and one patient showed valine heterozygosity. All patients showed type 1 PrP by Western blot analysis; nine cases were classified as MM1-type sCJD, and one case was classified as MV1-type sCJD (Table 1).

Neuropathologic findings

Six cases were classified as SSE, and four cases were classified as PE-type sCJD. There were no cases with Kuru plaques or florid plaques in the cerebrum or cerebellum. All cases fit the sCJD MM(MV)1 pathologic phenotype described by Parchi *et al.*[19] which is the typical sCJD pathology and includes a variable degree of spongiform degeneration with synaptic-type PrP deposition in the cerebral and cerebellar cortices. Pathology findings in the cerebrum, including the cortex and white matter, and the cerebellum, including the molecular, Purkinje neuron and granule cell layers and white matter, are listed in Table 2.

AQP-4 immunoreactivity in the cerebrum

AQP-4 immunoreactivity in control brains was restricted to the subpial zone (Fig. 1a) and subependymal zone. In SSE, strong AQP-4 immunoreactivity was observed predominantly in the cerebral cortex (Fig. 1b). In PE-type sCJD, widespread AQP-4 immunoreactivity was observed in the cerebral cortex and in the white matter (Fig. 1c). The hippocampus showed little AQP-4 immunoreactivity (Fig. 1d). Mild AQP4 immunoreactivity was detected around vessels in the control brain (Fig. 2a). AQP-4 immunoreactivity in the subpial and subependymal zones was stronger in sCJD than in the control brain (Fig. 2b,c). With regard to the cerebral cortex, no apparent AQP-4 immunoreactivity was observed in the control brain (Fig. 3a), whereas in SSE, many positive astrocytes were present (Fig. 3b). These astrocytes showed diffuse granular staining of the cell body and processes (Fig. 3c) and were suspected to be protoplasmic astrocytes due to their tufted morphology. In PE-type sCJD, numerous hypertrophic astrocytes were observed, and AQP-4 immunoreactivity was observed around the cell body and processes (Fig. 3d). Although widespread fine-vacuole type spongiform change was observed, particularly in the SSE cerebral cortex, no enhancement of AQP-4 immunoreactivity was observed in perivacuolar lesions compared to that in the neuropil. Furthermore, although numerous foamy macrophages were present, particularly in the cerebral white matter in PE-type sCJD, these macrophages did not show AQP-4 immunoreactivity. Corpora amylacea showed AQP-4 immunoreactivity, but neurons, microglial cells and oligodendrocytes did not.

Cerebellum							
Molecular layer			Purkinje neuron layer	Granule cell layer		White matter	
Pia matter and subpial zone	Around blood vessels	Parenchyma		Around blood vessels	Parenchyma	Around blood vessels	Parenchyma
+	+	+	±	+	±	+	−
+	+	+	±	+	±	±	−
++	++	++	++	++	++	+	−
++	+	+	+	+	+	±	−
++	+	±	±	+	±	±	−
++	+	+	+	+	+	±	−
++	++	++	+	+	+	+	±
++	++	++	+	+	+	+	±
+++	++	+++	++	++	++	±	−
+++	++	++	++	++	++	+	+
±	±	−	−	±	−	±	−
−	−	−	−	−	−	−	−

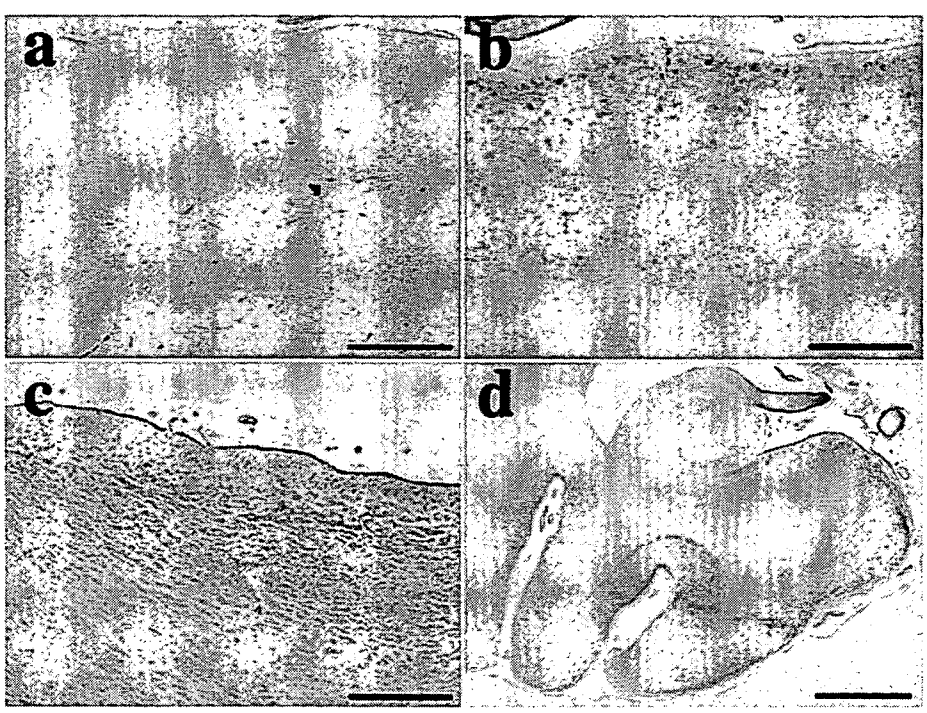

Fig. 1 Low-magnification images of cerebrum and immunolocalization of aquaporin-4 (AQP-4) in normal control, subacute spongiform encephalopathy (SSE) and panencephalopathic (PE)-type sporadic Creutzfeldt-Jakob disease (sCJD). (a) In normal control, AQP-4 immunoreactivity is restricted to superficial lesions. (b) In SSE, widespread immunoreactivity is present in the cerebral cortex. (c) In PE-type sCJD, the cerebral cortex and white matter show strong AQP-4 immunoreactivity. (d) The hippocampal formation shows little AQP-4 immunoreactivity. Bars: a–c, 1 mm; d, 5 mm, a–d, AQP-4 immunostaining: a, control; b and d, patient 1 (SSE case); c, patient 8 (PE-type sCJD case).

In the cerebral white matter, no immunoreactivity was observed in the control brain (Fig. 4a), weak immunoreactivity was observed only in perivascular lesions in SSE (Fig. 4b) and many hypertrophic astrocytes were immunoreactive in PE-type sCJD (Fig. 4c,d). However, some astrocytes, even hypertrophic astrocytes, lacked AQP-4 immunoreactivity.

AQP-4 immunoreactivity in the cerebellum

In the control brain, AQP-4 immunoreactivity was not observed in the cerebellar cortex or white matter (Figs 5a,6a). In SSE, the pia mater, subpial zone, molecular layer, Purkinje neuron layer and granule cell layer showed strong AQP-4 immunoreactivity (Fig. 5b), whereas the

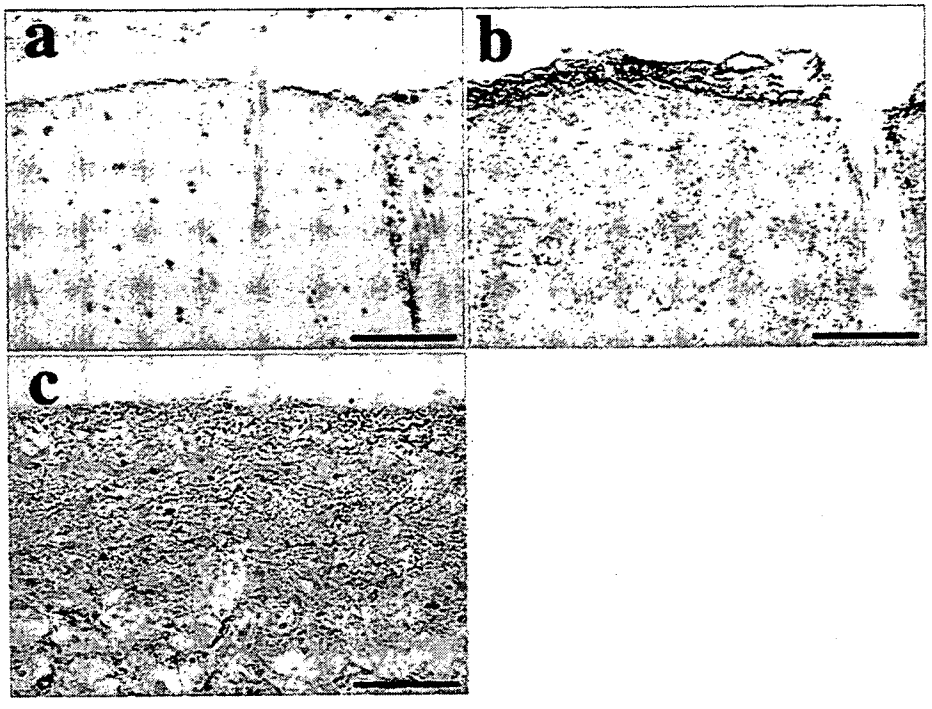

Fig. 2 Photomicrographs of superficial lesions of the cerebral cortex and immunolocalization of aquaporin-4 (AQP-4) in normal control, subacute spongiform encephalopathy (SSE) and panencephalopathic (PE)-type sporadic Creutzfeldt-Jakob disease (sCJD). (a) In normal control, AQP-4 immunoreactivity is restricted to the pia mater and around blood vessels. (b) In SSE, enhanced AQP-4 immunoreactivity is present in the pia mater and subpial zone compared to that in normal control. Moderate AQP-4 immunoreactivity is also detectable in the subpial gray matter and around blood vessels. (c) In PE-type sCJD, superficial lesions of the cerebral cortex show intense AQP-4 immunoreactivity. Bars: a–c, 100 m, a–c, AQP-4 immunostaining: a, control; b, patient 3 (SSE case); c, patient 9 (PE-type sCJD case).

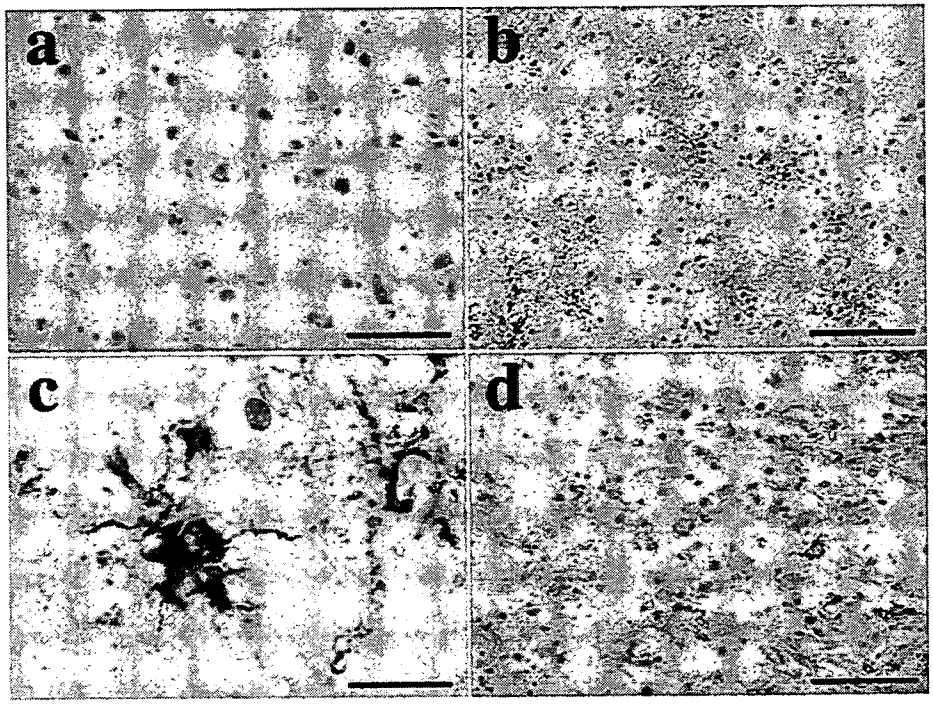

Fig. 3 Photomicrographs of cerebral neocortex and immunolocalization of aquaporin-4 (AQP-4) in normal control, subacute spongiform encephalopathy (SSE) and panencephalopathic (PE)-type sporadic Creutzfeldt-Jakob disease (sCJD). (a) In normal control, AQP-4 immunoreactivity is not apparent in the cerebral neocortex. (b) In SSE, immunoreactivity of many astrocyte cell bodies and processes is observed. (c) AQP-4 immunoreactivity is present in a diffuse granular pattern and shows tuft-like structures in the cell bodies and processes of protoplasmic astrocytes. (d) In PE-type sCJD, the cerebral neocortex shows strong AQP-4 immunoreactivity, although the lesion shows severe tissue rarefaction and status spongiosus. Bars: a, b, d, 100 m; c, 20 m, a–d, AQP-4 immunostaining: a, control; b and c, patient 1 (SSE case); d, patient 9 (PE-type sCJD case).

cerebellar white matter showed mild immunoreactivity only around blood vessels (Fig. 6b). In PE-type sCJD, moderate to strong AQP-4 immunoreactivity was observed, particularly in the atrophic molecular layer (Fig. 5c), and the cerebellar white matter showed no to mild immunoreactivity. Perivascular lesions showed little to mild AQP-4 immunoreactivity (Fig. 6c).

Relation between AQP-4 immunoreactivity, spongiform change, astrocytosis and GFAP and PrP immunoreactivity

Analysis of serial sections showed that spongiform change and gliosis in sCJD appeared at an earlier stage (Figs 7a1 and 8a1) than did strong AQP-4 immunoreactivity

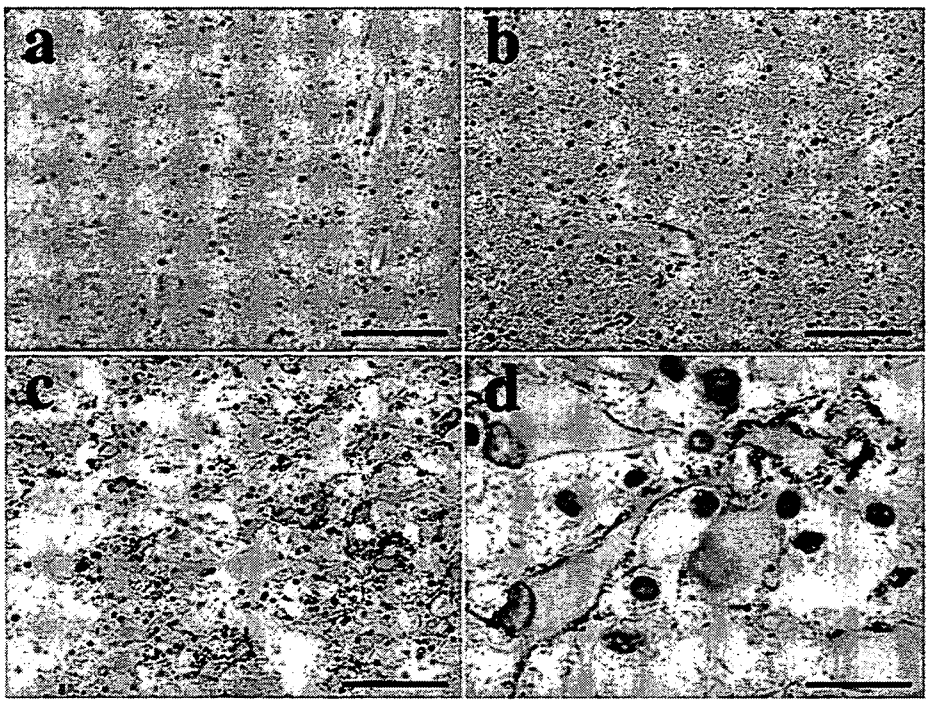

Fig. 4 Photomicrographs of cerebral white matter and immunolocalization of aquaporin-4 (AQP-4) in normal control, subacute spongiform encephalopathy (SSE) and panencephalopathic (PE)-type sporadic Creutzfeldt-Jakob disease (sCJD). (a) In normal control, AQP-4 immunoreactivity is not apparent in the cerebral white matter. (b) In SSE, weak immunoreactivity is detectable around blood vessels. (c) In PE-type sCJD, widespread strong AQP-4 immunoreactivity is observed around hypertrophic astrocytes. Some astrocytes, even hypertrophic astrocytes, lack AQP-4 immunoreactivity. Numerous foamy macrophages are also observed, but no AQP-4 immunoreactivity of these macrophages is observed. (d) AQP-4 immunoreactivity of hypertrophic astrocytes is present around cell bodies and their processes. In cell bodies and processes of hypertrophic astrocytes, no apparent AQP-4 immunoreactivity is observed. This pattern is different from that of positive astrocytes in SSE (see Fig. 3c). Bars: a–c, 100 m; d, 20 m; a–d, AQP-4 immunostaining: a, control; b, patient 1 (SSE case); c and d, patient 8 (PE-type sCJD case).

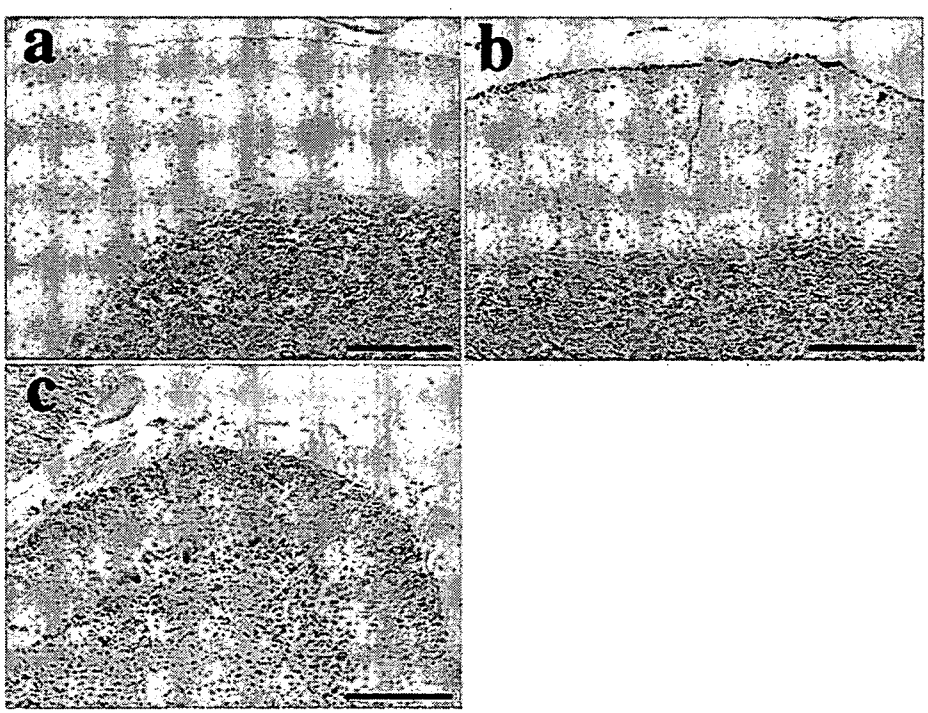

Fig. 5 Photomicrographs of cerebellar cortex and immunolocalization of aquaporin-4 (AQP-4) in normal control, subacute spongiform encephalopathy (SSE) and panencephalopathic (PE)-type sporadic Creutzfeldt-Jakob disease (sCJD). (a) In normal control, AQP-4 immunoreactivity is not apparent in the cerebellar cortex. (b) In SSE, widespread immunoreactivity is present in the pia mater, subpial zone, molecular layer, Purkinje neuron layer and granule cell layer. (c) In PE-type sCJD, strong AQP-4 immunoreactivity is observed, particularly in the atrophic molecular layer. Bars: a–c, 200 m; a–c, AQP-4 immunostaining: a, control; b, patient 3 (SSE case); c, patient 7 (PE-type sCJD case).

(Figs 7a3 and 8a3). Neuronal loss and tissue rarefaction in sCJD appeared at a later stage (Figs 7b1 and 8b1) than did strong AQP-4 immunoreactivity. Furthermore, strong AQP-4 immunoreactivity was present in burnt-out lesions (Figs 7b3 and 8b3) such as those in status spongiosus (Figs 7b1 and 8b1).

GFAP-positive astrocytes were present mainly in the superficial cortex in SSE (Fig. 7a2), whereas GFAP-positive astrocytes were widespread in the cerebral cortex and white matter in PE-type sCJD (Fig. 7b2). In serial sections, the distribution of GFAP-positive astrocytes in sCJD was different from that of AQP-4 immunoreactivity

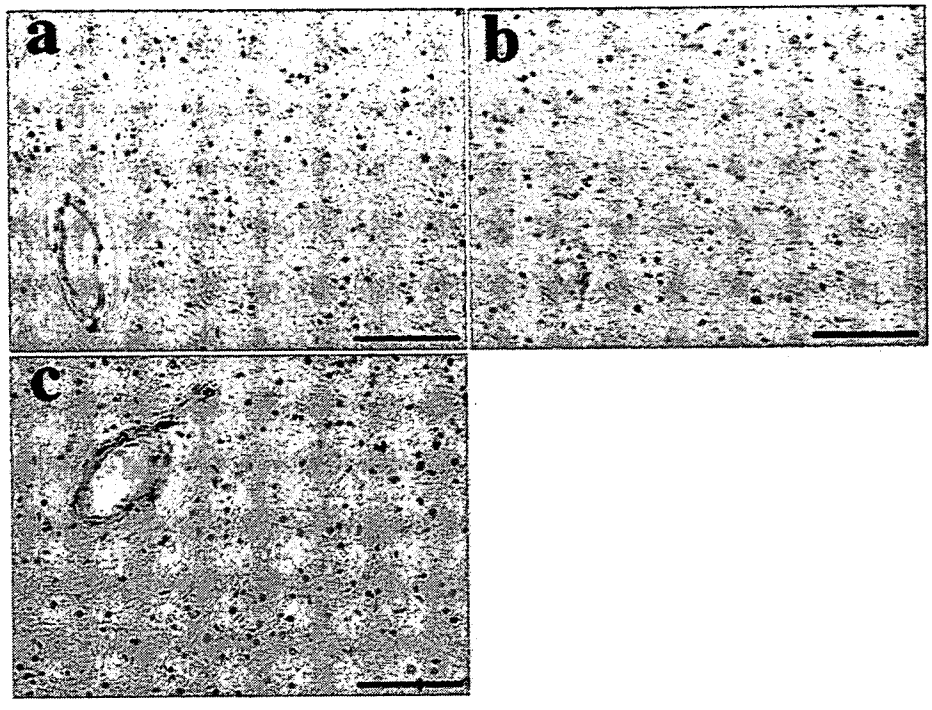

Fig. 6 Photomicrographs of cerebellar white matter and immunolocalization of aquaporin-4 (AQP-4) in normal control, subacute spongiform encephalopathy (SSE) and panencephalopathic (PE)-type sporadic Creutzfeldt-Jakob disease (sCJD). (a) In normal control, AQP-4 immunoreactivity is not apparent in the cerebellar white matter. (b) In SSE, weak immunoreactivity is present around blood vessels. (c) In PE-type sCJD, mild AQP-4 immunoreactivity is observed around blood vessels, but little AQP-4 immunoreactivity is observed in the cerebellar white matter. Bars: a–c, 100 m, a–c, AQP-4 immunostaining: a, control; b, patient 3 (SSE case); c, patient 7 (PE-type sCJD case).

(Fig. 7a2,a3,b2,b3). Strong AQP-4 immunoreactivity appeared at an earlier stage than did hypertrophic astrocytosis or GFAP-positive astrocytosis (Fig. 7a2,a3).

Widespread PrP deposition was observed in the cerebral and cerebellar cortices and appeared as fine granular and dot-like deposits (so-called synaptic-type accumulation[9,20]). No plaque-like deposits were identified, and the degree of PrP deposition varied between patients. In SSE, PrP deposition in the cerebral and cerebellar cortices was heavy (Fig. 8a2), and in PE-type sCJD, it was lighter (Fig. 8b2). PrP deposition in the cerebral white matter and cerebellar white matter was sparse or absent. In serial sections, the distribution of PrP deposition in sCJD was different from that of AQP-4 immunoreactivity (Fig. 8a2,a3,b2,b3). PrP deposition appeared at an earlier stage than did spongiform change or gliosis (Fig. 8a1,a2) and at an earlier stage than did strong AQP-4 immunoreactivity (Fig. 8a2,a3).

DISCUSSION

Increased AQP-4 immunoreactivity compared to that in controls was identified in all sCJD patients, as previously reported by our laboratory.[12] Rodriguez *et al.* reported increased AQP-4 expression in the cerebral cortex of 10 CJD patients (disease duration, 2–14 months) compared to that in age-matched controls by Western blot analysis.[13] The findings of the present study indicate that increased AQP-4 immunoreactivity is not restricted to the early stage of sCJD but also occurs at later stages. We speculate that the enhanced expression of AQP-4 in the sCJD brain reflects the intense astrocytosis associated with sCJD pathology. Enhanced expression of AQP-4 in patients with sCJD may not be a distinct pathologic entity but rather a secondary degenerative condition associated with sCJD pathology.

Intense astrocytosis is a pathologic feature of sCJD.[10] It is interesting that increased AQP-4 staining was observed in short disease duration SSE cases as well as prolonged disease cases of PE-type sCJD. Astrocytes are classified as protoplasmic or fibrous based on morphologic criteria, the former being found in normal gray matter, and the latter being found in normal white matter.[21] Interestingly, protoplasmic astrocytes showed AQP-4 immunoreactivity in SSE, whereas hypertrophic astrocytes showed AQP-4 immunoreactivity in PE-type sCJD in the present study.

Although the formation of and localized accumulation of abnormal PrP is considered to be a primary pathologic event in early stage sCJD,[22] the mechanism of neurodegeneration that accompanies this PrP accumulation remains unknown. Our results show that AQP-4 immunoreactivity occurs in the early stage of sCJD and remains until the prolonged disease stage. Investigation of AQP-4 immunoreactivity in the sCJD brain may aid in elucidating the relation between PrP deposition and the evolution of sCJD pathology. Although increased AQP-4 staining in the sCJD brain was observed, its relation to sCJD pathology is unknown. However, increased AQP-4 staining occurred after PrP deposition and before GFAP-positive hypertrophic astrocytosis. According to the results obtained with serial sec-